A new neornithischian dinosaur from the Upper Jurassic Tiaojishan Formation of northern China (#112698)

First submission

Guidance from your Editor

Please submit by **10 Feb 2025** for the benefit of the authors (and your token reward) .

Structure and Criteria
Please read the 'Structure and Criteria' page for guidance.

Custom checks
Make sure you include the custom checks shown below, in your review.

Author notes
Have you read the author notes on the guidance page?

Raw data check
Review the raw data.

Image check
Check that figures and images have not been inappropriately manipulated.

If this article is published your review will be made public. You can choose whether to sign your review. If uploading a PDF please remove any identifiable information (if you want to remain anonymous).

Files
Download and review all files from the materials page.

16 Figure file(s)
7 Table file(s)
1 Other file(s)

Custom checks

New species checks

- Have you checked our new species policies?
- Do you agree that it is a new species?
- Is it correctly described e.g. meets ICZN standard?

Structure and Criteria

Structure your review

The review form is divided into 5 sections. Please consider these when composing your review:

1. **BASIC REPORTING**
2. **EXPERIMENTAL DESIGN**
3. **VALIDITY OF THE FINDINGS**
4. General comments
5. Confidential notes to the editor

You can also annotate this PDF and upload it as part of your review

When ready submit online.

Editorial Criteria

Use these criteria points to structure your review. The full detailed editorial criteria is on your guidance page.

BASIC REPORTING

- Clear, unambiguous, professional English language used throughout.
- Intro & background to show context. Literature well referenced & relevant.
- Structure conforms to PeerJ standards, discipline norm, or improved for clarity.
- Figures are relevant, high quality, well labelled & described.
- Raw data supplied (see PeerJ policy).

EXPERIMENTAL DESIGN

- Original primary research within Scope of the journal.
- Research question well defined, relevant & meaningful. It is stated how the research fills an identified knowledge gap.
- Rigorous investigation performed to a high technical & ethical standard.
- Methods described with sufficient detail & information to replicate.

VALIDITY OF THE FINDINGS

- **Impact and novelty is not assessed.** Meaningful replication encouraged where rationale & benefit to literature is clearly stated.
- All underlying data have been provided; they are robust, statistically sound, & controlled.
- Conclusions are well stated, linked to original research question & limited to supporting results.

Standout reviewing tips

The best reviewers use these techniques

Tip	*Example*
Support criticisms with evidence from the text or from other sources	*Smith et al (J of Methodology, 2005, V3, pp 123) have shown that the analysis you use in Lines 241-250 is not the most appropriate for this situation. Please explain why you used this method.*
Give specific suggestions on how to improve the manuscript	*Your introduction needs more detail. I suggest that you improve the description at lines 57- 86 to provide more justification for your study (specifically, you should expand upon the knowledge gap being filled).*
Comment on language and grammar issues	*The English language should be improved to ensure that an international audience can clearly understand your text. Some examples where the language could be improved include lines 23, 77, 121, 128 – the current phrasing makes comprehension difficult. I suggest you have a colleague who is proficient in English and familiar with the subject matter review your manuscript, or contact a professional editing service.*
Organize by importance of the issues, and number your points	*1. Your most important issue* *2. The next most important item* *3. …* *4. The least important points*
Please provide constructive criticism, and avoid personal opinions	*I thank you for providing the raw data, however your supplemental files need more descriptive metadata identifiers to be useful to future readers. Although your results are compelling, the data analysis should be improved in the following ways: AA, BB, CC*
Comment on strengths (as well as weaknesses) of the manuscript	*I commend the authors for their extensive data set, compiled over many years of detailed fieldwork. In addition, the manuscript is clearly written in professional, unambiguous language. If there is a weakness, it is in the statistical analysis (as I have noted above) which should be improved upon before Acceptance.*

A new neornithischian dinosaur from the Upper Jurassic Tiaojishan Formation of northern China

Yunfeng Yang [1, 2], **James L King** [2, 3], **Xing Xu** [Corresp. 2, 4]

[1] College of Earth and Planetary Sciences, University of Chinese Academy of Sciences, Beijing, China

[2] Institute of Vertebrate Paleontology and Paleoanthropology, Chinese Academy of Sciences, Beijing, China

[3] Colorado Northwestern Community College, Craig, Colorado, United States

[4] Centre for Vertebrate Evolutionary Biology, Yunnan University, Kunming, China

Corresponding Author: Xing Xu
Email address: xu.xing@ivpp.ac.cn

The Middle and Late Jurassic Yanliao Biota is different from other contemporaneous fossil assemblages in that it lacks neornithischian dinosaurs. Here, we report a new, early-diverging neornithischian, *Pulaosaurus qinglong* gen.et sp. nov. , from the Upper Jurassic Tiaojishan Formation of Qinglong, Hebei Province, of northern China. Diagnostic or noteworthy morphological characteristics of *P. qinglong* include: five premaxillary teeth; a small boss on the posteroventral corner of the jugal dorsal ramus; a nuchal crest is located on the parietal; the squamosal forms a glenoid facet that articulates with the quadrate; a foramen along the coracoid is absent; the manus has five digits; a supra-acetabular crest is observable on the ilium; a pair of gracile, leaf-like arytenoids; the obturator process along the ischium is located near the pubic peduncle; a notch-like shape forms the obturator opening in the pubis; a subtriangular flange extends dorsolaterally along four distal tarsals; three of the distal tarsals are unfused, including a small drop-shaped distal tarsal 3; distal tarsal 3 is pierced by a foramen. A phylogenetic analysis places *P. qinglong* as one of the earliest-diverging neornithischians yet described. Moreover, *P. qinglong* represents the second known dinosaur to preserve ossified laryngeal elements, thus suggesting that a bird-like vocalization evolved early in dinosaur evolution.

A new neornithischian dinosaur from the Upper Jurassic Tiaojishan Formation of northern China

Yunfeng Yang[1,2], James Logan King[1,3], Xing Xu[1,4]

[1] Institute of Vertebrate Paleontology and Paleoanthropology, Chinese Academy of Sciences, Beijing, 100044, China
[2] College of Earth and Planetary Sciences, University of Chinese Academy of Sciences, Beijing, 100049, China
[3] Colorado Northwestern Community College, Craig, Colorado, 81625, United States
[4] Centre for Vertebrate Evolutionary Biology, Yunnan University, Kunming, Yunnan, 650091, China

Corresponding Author:
Xing Xu
No.142 Xizhimen outer Street, Beijing, 100044, China
Email address: Xing Xu, xuxing@ivpp.ac.cn

Abstract

The Middle and Late Jurassic Yanliao Biota is different from other contemporaneous fossil assemblages in that it lacks neornithischian dinosaurs. Here, we report a new, early-diverging neornithischian, *Pulaosaurus qinglong* gen.et sp. nov., from the Upper Jurassic Tiaojishan Formation of Qinglong, Hebei Province, of northern China. Diagnostic or noteworthy morphological characteristics of *P. qinglong* include: five premaxillary teeth; a small boss on the posteroventral corner of the jugal dorsal ramus; a nuchal crest is located on the parietal; the squamosal forms a glenoid facet that articulates with the quadrate; a foramen along the coracoid is absent; the manus has five digits; a supra-acetabular crest is observable on the ilium; a pair of gracile, leaf-like arytenoids; the obturator process along the ischium is located near the pubic peduncle; a notch-like shape forms the obturator opening in the pubis; a subtriangular flange extends dorsolaterally along four distal tarsals; three of the distal tarsals are unfused, including a

small drop-shaped distal tarsal 3; distal tarsal 3 is pierced by a foramen. A phylogenetic analysis places *P. qinglong* as one of the earliest-diverging neornithischians yet described. Moreover, *P. qinglong* represents the second known dinosaur to preserve ossified laryngeal elements, thus suggesting that a bird-like vocalization evolved early in dinosaur evolution.

Introduction

The Middle-to-Late Jurassic-aged Yanliao Biota is one of the most significant Mesozoic, terrestrial lagerstätte in China (Bai 2024; Huang 2015; Liu 2022; Zhou & Wang ~~2017) and is~~ comprised of fossil assemblages from the Jiulongshan and the Tiaojishan Formations (Boyd 2015; Huang 2015; Zhou & Wang 2017). The Daohugou Biota represents its earliest stage while the Linglongta Biota represents its late stage (Huang 2015; Zhou & Wang 2017). In total, there have been 54 genera and 58 species of vertebrates reported from the Yanliao Biota, including 9 species of non-avian dinosaurs (Liu 2022; Zhou & Wang 2017). Because it preserves large amounts of vertebrate material from many taxa, the Yanliao Biota offers insight to major palaeobiological events, such as the temporal origin of birds and the early evolution of mammals (Liu 2022; Xu et al. 2022; Zhou & Wang 2017). However, non-avian dinosaurs found in the Yanliao Biota are all small-bodied theropods ~~and Ornithischia~~ is represented by only one species, which may possibly be from Jehol Biota (Zhou & Wang 2017). This is in stark contrast to other contemporaneous Chinese terrestrial faunas such as the Shishugou and Shaximiao faunas where body size and taxonomic composition ~~is~~ more varied (Liu 2022; Xu et al. 2022).

Here, we describe a new ~~neornthischian~~ specimen found in the Upper Jurassic Tiaojishan Formation, County Qinglong, Province Hebei, China. This well-preserved specimen(IVPP V30936) has both basal and derived characteristics of Ornithischia and preserves cololites,

hyoids, and an ossified larynx. This new neornithischian specimen helps us understand the biodiversity of Yanliao Biota better.

Institutional abbreviations

IVPP: Institute of Vertebrate Paleontology and Paleoanthropology, Beijing, China

Materials & Methods

The specimen V30936 was acquired from the locals, which was found in Southern Shimen Gou, County Qinglong, Province Hebei, People's Republic of China. The specimen is fully prepared. Based on close examinations and comparations, its authenticity is guaranteed.

The anatomical information of IVPP V30936 was acquired by personal observations. They were supplemented by computed tomography (CT) scans of the pelvic girdle. The CT scans were conducted by 160-Micro-CL（Computed Laminography）in IVPP. The CT data provides insight into areas of the pelvic girdle obscured by the femora and the chevrons to gain more complete anatomical data onIVPP 30936.

Phylogenetic Analysis

To assess the phylogenetic position of IVPP V30936 within ornithischians, we ran the phylogenetic analysis on the emended matrix dataset ~~of Han et al. in 2017 (Han 2017)~~ with IVPP V30936 and *Sanxiasaurus modaoxiensis*, a recently reported early-diverging neornithischian taxon, ~~added to the dataset~~. The coding of *Sanxiasaurus* was based on the description and images ~~provided by Ning Li (Li et al. 2019).~~ For consistency, we followed the phylogenetic nomenclature of higher-level ornithischian taxa as defined by Madzia et al. (Madzia et al., 2021).

The final dataset consists of 380 characters scored for 70 ingroup taxa and 4 outgroup taxa. The analysis was conducted on TNT with each character equally weighted. The analysis is based on the traditional search with 1000 random seeds and 1000 replications. The swapping algorithm is tree bisection reconnection (TBR), with 100 trees to save per replication. The maximal memory of trees was set to 100000 and zero-length branches collapsed.

Unstable taxa were identified by the command 'pruned trees' up to seven taxa, including *Pisanosaurus*, *Sanxiasaurus*, *Micropachycephalosaurus*, *Zephylosaurus*, *Yueosaurus*, *Yandusaurus* and *Gasparinisaura*. Having removed the unstable taxa from the most parsimonious tree topology, the reduced strict consensus tree shows the phylogenetic relationships of the remaining taxa.

Results

Systematics Paleontology

Dinosauria Owen, 1842

Ornithischia Seeley, 1887

Neornithischia Cooper, 1985 (sensu, Sereno, 1998)

Pulaosaurus qinglong gen.et sp. nov.

Etymology

The generic name is derived from Chinese Pinyin for "Pulao", a mythical creature similar to the Chinese dragon that is good at shouting in Chinese legends, as it's associated with a possible bird-like vocalizations of this species. The specific name is derived from "Qinglong", which is the name of the county in Province Hebei, China, where the specimen was found, in Chinese Pinyin.

Holotype

IVPP V30936 is comprised of a nearly complete skeleton on a brownish-red sandstone slab. The specimen preserves most of the skull and a complete postcranial skeleton. Many skull elements are displaced and disarticulated due to mediolateral crushing. Cervical vertebrae and dorsal vertebrae are compressed and obscured. The sacrum is overlapped by the ilium. Only two anterior, five middle and seventeen posterior caudal vertebrae are preserved well. Both scapulae and the sternum are broken with only fragments preserved. The left forelimb is complete and is articulated while the right humerus is not preserved and elements of the right manus are disarticulated. The pelvic girdle elements are preserved although many morphological characters are unknown due to overlapping and displaced elements. Most of the hindlimbs are preserved except for the right distal tarsal 2, 3, 4, left calcaneum, and the phalange 1 of the left pes. Additionally, a pair of ceratobranchials and ossified arytenoids are also preserved ventrally adjacent to the mandible. Cololites are preserved in the abdominal cavity.

Locality and Horizon

Southern Shimen Gou, County Qinglong, Province Hebei, People's Republic of China.

Tiaojishan Formation, Callovian-Oxfordian (Middle-Upper Jurassic)

Diagnosis

A small-body neornthischian dinosaur characterized by the combination of the following characteristics (autapomorphies preceded by an asterisk): five premaxillary teeth; a small boss on the posteroventral corner of the jugal dorsal ramus; a nuchal crest on the parietal; the squamosal

126 forms a glenoid facet that articulates with the quadrate; *a coracoid foramen is absent; the manus
127 has five digits; a supra-acetabular crest is located on the ilium; a pair of gracile, leaf-like
128 arytenoids are present; the obturator process is near the pubic peduncle; the opening of the
129 obturator on the pubis is notch-shaped; a subtriangular flange extends dorsolaterally on four
130 distal tarsals; *three distal tarsals are unfused with distal tarsal 3 that is drop-shaped; distal tarsal
131 3 is pierced by a foramen.

132 *Pulaosaurus qinglong* differs from *Agilisaurus louderbacki* in the following characteristics:
133 the relative length of the *Pulaosaurus* skull is more elongated while the skull of *Agilisaurus* is
134 foreshortened; the maxillary process of the premaxilla contacts the lacrimal in *Pulaosaurus* while
135 the maxillary process of the premaxilla does not contact the lacrimal in *Agilisaurus*; premaxillary
136 teeth in *Pulaosaurus* are subequal to each other while the middle premaxillary teeth are largest in
137 *Agilisaurus*; a small boss is present on the jugal of *Pulaosaurus* while there is no ornamentation
138 on the jugal of *Agilisaurus*; the ventral edge of the *Pulaosaurus* jugal is straight while the ventral
139 edge of the *Agilisaurus* jugal deflects posteroventrally; the squamosal forms a glenoid on the
140 quadrate process with the dorsal squamosal surface being flat and is expanded laterally in
141 *Pulaosaurus* while the glenoid is absent in *Agilisaurus*; the ventral process of the predentary is
142 notably reduced in *Pulaosaurus* when compared to that of *Agilisaurus*; the ossified tendons of
143 *Pulaosaurus* are in basket-like arrangement of fusiform tendons in caudal region while they are
144 arranged longitudinally in *Agilisaurus*; manual digit I ungual is sub-conical in *Pulaosaurus* while
145 it is claw-like in *Agilisaurus*; the obturator foramen in the pubis is a notch-like shape in
146 *Pulaosaurus* while it is a foramen in *Agilisaurus*; the ischial obturator process is near the pubic
147 peduncle in *Pulaosaurus* while it is far from the pubic peduncle in *Agilisaurus*; there are three
148 distal tarsals in *Pulaosaurus* while there are only two ones in *Agilisaurus*.

Pulaosaurus qinglong differs from *Hexinlusaurus multidens* in the following characteristics: the maxillary process of the premaxilla contacts the lacrimal in *Pulaosaurus* while the maxillary process of the premaxilla does not contact the lacrimal in *Hexinlusaurus*; a small boss is present on the jugal of *Pulaosaurus* while there is no ornamentation on the jugal of *Hexinlusaurus*; the orbital margin of the postorbital ~~is~~ does not project in *Pulaosaurus* while it projects into the orbit in *Hexinlusaurus*; the frontals of *Pulaosaurus* are shorter and more elongated than those of *Hexinlusaurus*; the squamosal forms a glenoid on the quadrate process with the dorsal surface flat and expanded laterally in *Pulaosaurus* while the glenoid is absent in *Hexinlusaurus*; ossified tendons of *Pulaosaurus* are in basket-like arrangement of fusiform tendons in caudal region while they are arranged longitudinally in *Hexinlusaurus*; the ratio between the humerus and the femur in *Pulaosaurus* is shorter than that of *Hexinlusaurus*; the ungual of manual digit I is sub-conical in *Pulaosaurus* while it is claw-like in Hexinlusaurus; there is a supra-acetabular crest on the ilium of *Pulaosaurus* that is absent in *Hexinlusaurus*; the obturator foramen of the pubis is a notch in *Pulaosaurus* while it is a foramen in *Hexinlusaurus*; the ischial obturator process is near the pubic peduncle in *Pulaosaurus* while it is far from the pubic peduncle in *Hexinlusaurus*; the astragalar ascending process is triangular in *Pulaosaurus* while it is finger-like in *Hexinlusaurus*.

Description and comparisons

The specimen is preserved on a brownish-red fine-grained sandstone slab（FIGURE 1） and is roughly mediolaterally compressed. The total length of this specimen is about 722mm while its skull length is about 8cm and the length of trunk (i.e. the length from the atlas to the

posterior border of the pelvic girdle) is about 30cm. The neurocentral sutures of cervical and caudal vertebrae are visible (FIGURE 5, 7), suggesting that it is an immature individual.

Skull

In lateral view, its skull shape（FIGURE 2, 3） is an elongate, low, and obtuse triangle. Due to the displacement of the jugal, the exact position of postorbital bones and the shape of infratemporal fenestra remain unknown. The supratemporal fenestra is sub-square in outline from lateral view. The orbit is elliptical and is the largest cranial opening with a maximal diameter of ~~which is~~ about 3cm. The ratio between the maximal diameter of the orbit and skull length is about 36%, a ratio similar to larger individuals of *Jeholosaurus* (Barrett 2009). Anterior to the orbit sits the subtriangular antorbital fossa seen in most early-diverging ornithischians including *Jeholosaurus*, *Lesothosaurus*, *Hexinlusaurus*, *Agilisaurus* (David B. Norman et al. 2004; Paul M. Barrett 2009; Peng 1992; Sereno 1991; Xinlu He et al. 1984), whose ventral margin is delineated nearly at the same horizon of orbit ventral margin. Mandibular elements are disarticulated from each other, so the exact overall shape of the mandible and the presence or shape of external mandibular fenestra is unknown.

Premaxilla (FIGURE 2)—Only the left premaxilla is visible ~~in~~ the lateral view of this specimen. In lateral view, the main body of the premaxilla is subrectangular and possesses two processes: a tapering and caudodorsal-oriented maxillary process that forms the ventral border of the external nares and a reduced nasal process that forms the anterior border of the external nares. The ventral margin of the premaxilla is ventrally offset ~~to~~ the maxilla's ventral margin as seen in many ornithopods, which is a plesiomorphy ~~in~~ neornithischians (Norman et al. 2004). In lateral view, the nasal process of the premaxilla is reduced and does not contact the nasals, possibly due to damage. The maxillary process of the premaxilla contacts the lacrimal with its caudal border

194 contacting the maxilla and with the rostrodorsal border contacting the nasal, excluding the
195 maxilla from contacting the nasal, which is a synapomorphy of *Changmiania* (Yang et al. 2020)
196 and *Jeholosaurus* (Barrett 2009). The main body of the premaxilla is dorsoventrally concave
197 with its caudal margin being more dorsoventrally convex. The lateral surface of the premaxilla's
198 main body is moderately concave, where it flares and thickens along the oral margin. Rostral to
199 the first premaxillary tooth, a short edentulous region develops into a hook-shaped projection.
200 The rostral margin of the premaxillary main body is rugose, suggesting the presence of a
201 rhamphotheca ~~on the premaxilla~~, which is a plesiomorphy among neornithischians as observed in
202 *Lesothosaurus* (Sereno 1991), *Jeholosaurus* (Barrett 2009), *Changchunsaurus* (Jin et al. 2010),
203 *Hypsilophodon* (Norman et al. 2004). The fossa-like depression along the premaxilla-maxilla
204 boundary is absent, which is a synapomorphy in *Haya* (Berta 2021), *Orodromeus* (Scheetz
205 1999), *Jeholosaurus* (Barrett 2009) and *Changchunsaurus* (Jin et al. 2010). There is no arched
206 diastema between the premaxilla and the maxilla, a synapomorphy usually seen in within
207 Heterodontosauridae (Norman et al. 2004). A premaxilla foramen is also absent, a
208 synapomorphy observed in *Haya* (Berta 2021), *Orodromeus* (Scheetz 1999), *Jeholosaurus*
209 (Barrett 2009), *Changchunsaurus* (Jin et al. 2010) and *Agilisaurus* (Peng 1992). Moreover, there
210 is no prominent narial fossa and the ventral region of the premaxilla does not flare laterally to
211 form the floor of the narial fossa. These morphological characters suggest the premaxilla of
212 *Pulaosaurus* resembles that of early-diverging neornithischians.
213 Five bulbous and unserrated premaxillary teeth are present, the same number as *Haya* (Berta
214 2021), *Orodromeus* (Scheetz 1999), *Changchunsaurus* (Jin et al. 2010), but different from the
215 six found in *Jeholosaurus* (Barrett 2009), *Lesothosaurus* (Sereno 1991) and *Agilisaurus* (Peng
216 1992); four in *Convolosaurus marri* (Forster et al. 2019); or none in *Tenontosaurus tilletti*

(Winkler & Murry 1997). The premaxillary tooth number of *Pulaosaurus* is rather primitive compared to later-diverging ~~taxa of Neornithischia but is derived~~ than tooth counts of most early-diverging taxa within Neornithischia. The first premaxillary tooth is close to the tip of the premaxilla and the second tooth. The first premaxilla tooth is moderately smaller than the following four teeth which are all subequal in size ~~to each other~~. In lateral view, the premaxillary tooth crown is recurved while the root is long and straight, with the crown moderately expanding above the root. The overall premaxilla tooth shape of *Pulaosaurus* resembles that of *Agilisaurus* (Peng 1992), a plesiomorphy in early-diverging neornithischians. The crown is recurved and spade-shaped while the root is long and straight, with the crown moderately expanded above the root. The labial surface is smooth, and no obvious carinae are visible. There are wear facets on the posterior surfaces of the labial side on the 2nd, 3rd, and 5th premaxillary tooth. The premaxillary tooth row is offset laterally from the maxillary tooth row. No obvious diastema is present between the premaxillary tooth row and the maxillary tooth row.

Maxilla—The left maxilla is preserved in lateral view. It is an elongate, plate-like, trapezoidal bone consisting of a straight, tooth-bearing ramus and an ascending process. The tooth-bearing ramus widens mediolaterally from anterior to posterior while the thin and dorsally ascending process arises from the rostro-dorsal region of the element where it contacts the lacrimal dorsally. The premaxilla overlaps the rostral region of the maxilla, so the ascending process is not fully exposed. The maxilla forms the ventral border of the subtriangular antorbital fossa. Due to taphonomic compression, it is unknown whether additional openings within the antorbital fossa are present or not. It is also unknown whether the anterolateral boss articulating with the

premaxilla is present or not because the anterior region is overlapped by the premaxilla. The maxillary fenestra is absent. There is no slot in the maxilla for lacrimal. Rostro-caudally, the tooth-bearing ramus thickens, forming a ridge. The ridge starts from the 7th maxillary tooth and extends laterodorsally with its caudal end tapering and flaring laterally. The tooth row is medially inset to form a buccal emargination as seen in most ornithischians (Norman et al. 2004), which is a plesiomorphy in neornithischians (Norman et al. 2004). Three or four probable nutrient foramina lie on the maxillary lateral surface. It is uncertain how many existed in life due to poor preservation（FIGURE 2）.

There are 10 maxillary teeth observed in this specimen, ~~with~~ all in labial view. Except for the 8th replacement tooth, the apicobasal and mesiodistal lengths of the teeth increase from the mesially located teeth to the central tooth before declining distally. Each maxillary tooth is subtriangular with a distinct neck and a cingulum between the crown and the root, similar to many early-diverging ornithischians (Norman et al. 2004; Peng 1992; Sereno 1991; He et al. 1984). The labial surfaces of the maxillary teeth are relatively smooth with worn faces but no apicobasally extending ridges are observed in *Jeholosaurus* (Barrett 2009), *Changchunsaurus* (Jin et al. 2010), ~~or~~ *Lesothosaurus* (Norman et al. 2004), *Tenontosaurus* (Winkler & Murry 1997). The mesial and distal margins of the teeth are ornamented with simple denticles as observed in *Jeholosaurus* (Barrett 2009), *Lesothosaurus* (Norman et al. 2004), and *Agilisaurus* (Peng 1992)~~, as this is considered a plesiomorphy in neornithischians. In overall morphology~~, the maxillary teeth of *Pulaosaurus* resemble those of early-diverging ornithischians.

Nasal—The left nasal is taphonomically compressed with its rostral end broken, so the internarial bar is not preserved. It is unknown whether both nasals were fused or not in life. In

lateral view, the left nasal is hatchet-shaped with a tapering and posterodorsally extending caudal process forming the dorsal border of the external nares. The main body of the nasal ventrally contacts the subnarial process of the premaxilla while its caudal process contacts the lacrimal ventrally, overlapping the prefrontal. It appears that the nasals were excluded from the antorbital fossa. No obvious narial fossa or nasal foramina is observed in the specimen.

Lacrimal— In lateral view, the lacrimal is an inverted L-shaped bone comprising the robust rostrodorsal process and the thin caudoventral process. The lacrimal forms the dorsal border of the antorbital fossa. Its dorsal margin contacts the nasal anterodorsally and contacts the prefrontal posterodorsally. The lacrimal's anteroventral corner contacts the premaxilla, the maxilla and its ventral border overlaps the palatine. The tip of the lacrimal's caudoventral process is situated anterior to the jugal and posterodorsal to the maxilla.

Prefrontal— In lateral view, the left prefrontal is a rod-like bone which anteriorly contacts the lacrimal and the nasal and overlaps the frontal caudally while forming the anterodorsal margin of the orbit. On its rostral end, the prefrontal has a descending ventral process that rostrally articulates with the rod-like palpebral.

Palpebral— The left palpebral is preserved in the specimen. Similar to most ornithischians(Norman et al. 2004), the palpebral of *Pulaosaurus* is a rod-like bone with its rostral end articulating with the prefrontal and the frontal In IVPP V30936, the caudal end of the palpebral is overlapped by the displaced jugal. Its length is more than 80% of the orbit diameter and its caudal end projects into the orbit freely, which is different from other ornithischians such

as *Huayangosaurus taibaii* (Galton & Upchurch 2004) where the palpebral is incorporated into the orbit margin, which is a plesiomorphy of neornithischians. The palpebral does not articulate with the postorbital as seen in *Agilisaurus* (Peng 1992; He et al. 1984). There is no trace of postpalpebral observed in *Haya* (Berta 2021) or *Thescelosaurus* (Boyd 2014).

Jugal— The left jugal is preserved, though it is taphonomically displaced. In lateral view, the jugal is a plate-like bone composed of three rami and it forms the posteroventral border of the orbit and the anteroventral border of the infratemporal fenestra. Due to its displacement, its contact with other bones remains uncertain. Different from *Yinlong* (Han 2017), the jugal is excluded from the antorbital fossa as observed in *Jeholosaurus* (Barrett 2009), *Haya* (Berta 2021), *Hexinlusaurus* (He et al. 1984), and *Agilisaurus* (Peng 1992), which is a plesiomorphy in neornithischians. The anterior process is dorsoventrally thin and narrow. Similarly, the dorsal process is slender and thin. Due to displacement, the jugal's articulating surface with the postorbital is exposed. There is a small boss on the posteroventral corner of the jugal, which is similar to *Orodromeus* (Scheetz 1999) but much smaller. Similar nodular ornament is a synapomorphy that is present in *Orodromeus* (Scheetz 1999), *Heterodontosaurus* (Jin et al. 2010), *Zephyrosaurus* (Jin et al. 2010), and marginocephalians (Jin et al. 2010) but absent in Ornithopoda (Jin et al. 2010). It is possible that the size of jugal boss is ontogenetically variable as in *Orodromeus* (Scheetz 1999). The posterior process of the jugal is lateromedially thin, plate-like and bifurcated, which is weakly expanded posterodorsally. A bifurcated posterior process is a synapomorphy present in *Lesothosaurus* (Norman et al. 2004), *Jeholosaurus* (Barrett 2009), *Changchunsaurus* (Jin et al. 2010), and psittacosaurs (Hailu You & Dodson 2004) ~~but is~~ absent in *Agilisaurus* (Peng 1992) and many early-diverging cerapodans – including *Hypsilophodon*

(Jin et al. 2010), pachycephalosaurs (Jin et al. 2010) and *Yinlong* (Jin et al. 2010). There is no ornamentation on the lateral side of the ~~jugal similar to that of~~ *Jeholosaurus* (Barrett 2009).

Frontal— In lateral view, the left frontal is an elongate and dorsoventrally thick arched shelf that forms the anterodorsal roof the skull. The anterodorsal margin articulates with the prefrontal, the anteroventral corner articulates with the palpebral, and it posteriorly contacts the parietal. The frontal is elongated and narrow, a synapomorphy in early-diverging neornithischians (Barrett 2009) . Although the exact ratio between its length and width is unknown, the value is estimated to be about 2.5 based. The estimated length and width ratio is smaller than that of *Jeholosaurus* (Barrett 2009), *Agilisaurus* (Peng 1992), *Hypsilophodon* (Barrett 2009), and *Zephyrosaurus* (Jin et al. 2010) but greater than that of early-diverging ceratopsians (Barrett 2009), *Hexinlusaurus* (Barrett 2009), *Orodromeus* (Scheetz 1999) and *Thescelosaurus* (Berta 2021; Barrett 2009). The lateral margin thins and flares laterally, forming the orbital margin. The orbital margin is not as rugose as other ornithischians. There exists a groove on the anterodorsal margin of the ~~orbital margin~~ that articulates with the prefrontal and curves ventrally. The dorsal margin of the frontal thins and projects posterodorsally, which makes the dorsal margin convex and highest over the orbit. The suture between the frontal and the parietal is a short scarf-joint lying moderately behind the orbit, with the posterior margin of the frontal overlapped by the parietal.

Postorbital— In lateral view, the postorbital is a triradiate-shaped bone composed of an infratemporal process that extends anterodorsally, a jugal process that extends anteroventrally, and a squamosal process that extends posteriorly. The surface of the postorbital is smooth and lacks ornaments on its surface, which is a plesiomorphy of early-diverging neornithischians including *Jeholosaurus* (Barrett 2009), *Haya* (Berta 2021), and *Orodromeus* (Scheetz 1999). The

orbital margin of the postorbital does not project into orbit as in *Haya* (Berta 2021) and *Orodromeus* (Scheetz 1999), a plesiomorphy of neornithischians. The anterior end of the infratemporal process is broken but would have been longer than the squamosal process and would have articulated with the posteroventral corner of the frontal. The squamosal process is short and tapers into a narrow tip where it articulates with the squamosal ventrally. The length of the squamosal process suggests that the anteroposterior length of infratemporal fenestrae is relatively short. The jugal process is overlapped by the quadrate, so its specific morphological characters remain unknown. However, based on the morphology of the jugal's dorsal process, the anteroposterior width of the jugal process of the postorbital decreases and it articulates with the jugal with a scarf-joint.

Parietal— In lateral view, the left parietal is a saddle-shape bone, which forms the posterodorsal roof of the skull and the infratemporal fenestrae. It contacts the frontal anteriorly along with the postorbitals and the squamosals laterally. Its posterior margin flares laterally to form the nuchal crest, ~~a synapomorphy also observed~~ in *Haya* (Berta 2021), *Changmiania* (Yang et al. 2020), *Orodromeus* (Scheetz 1999), and *Oryctodromeus* (Krumenacker 2017). It forms the posterior margin of the supratemporal fenestrae. It is unknown whether a sagittal crest or a median process inserts between the frontals.

Squamosal— In lateral view, although overlapped by the squamosal process of the postorbital, the squamosal is a small and triradiate bone has had its quadrate ramus broken away. The dorsal surface of the squamosal is smooth and flares laterally to form a glenoid on the quadrate ramus to articulate with the quadrate, as observed in early-diverging ceratopsians such as *Yinlong* (You

& Dodson 2004), *Hualianceratops* (You & Dodson 2004), and *Liaoceratops* (You & Dodson 2004), suggesting that this synapomorphy of ceratopsians is present much earlier in neornithischians. The posterior ramus is visible in anterolateral view and has a concavity formed by its lateral surface. Its contacting relationships with other bones remain uncertain due to the displacement of bones.

Quadrate— The left quadrate is exposed in lateral view. Two-thirds of the quadrate shaft is bowed posteriorly. The quadrate head is bluntly round. The quadrate articulates with the squamosal and its distal condyle is overlapped by the pterygoid. Due to displacement, its exact contact relationships with other cranial bones remains unknown. The shaft flares laterally to form the anterolateral-oriented jugal wing. The jugal wing of the quadrate arises from the dorsal margin and terminates just above the distal condyle. The pterygoid wing and the distal condyle are overlapped, so their morphological characteristics are unknown. However, it could be determined if the quadrate condyle is ventrally offset to the level of the maxillary tooth row. It could not be determined whether a quadrate foramen is present or not.

Quadratojugal— In lateral view, the left quadratojugal is a subtriangular and flat bone which is overlapped by the jugal with its ventral margin covered by the ectopterygoid. The quadratojugal is comprised of a relatively long dorsal process, an anterior process, and a short posteroventral process. The dorsal process and the anterior process are not as long, ~~relatively speaking,~~ as those of *Gasparinisaura* (Coria 1996). Due to displacement, the relationship ~~with~~ the quadratojugal and ~~with~~ other cranial elements remains unknown. Due to overlapping elements, it cannot be

determined whether a quadratojugal foramen is present as is observed in neornithischians such as *Hypsilophodon* (Norman et al. 2004), *Jeholosaurus* (Barrett 2009).

Pterygoid— In lateral view the medial side of the right pterygoid is exposed due to displacement. The pterygoid consists of three processes: the quadrate process, the mandibular process, and the palatine process. The quadrate process is a thin, subtriangular sheet that projects posterodorsally and is comparably much smaller than that of *Thescelosaurus* (Boyd 2014). Medially, a posteromedially facing cup-shape arises from the anterior corner of the quadrate process where it joins with the other processes. The mandibular process is a thin, small, anteroposteriorly long, and subtriangular sheet that projects ~~dorsally that arises~~ from the posterior corner of the quadrate process. The palatine process originates from the posteromedially facing cup-shape, ~~extends anteriorly and tapers anteriorly while it expands lateromedially and forms a tab that is lateromedially oriented.~~ This tab is much shorter relative to the one ~~in~~ found on the pterygoid's palatine process of *Thescelosaurus* (Boyd 2014).

Ectopterygoid— In lateral view, ~~it~~ is a small bar with a notch on the dorsal margin that extends posteroventrally where it is posteriorly close to the caudal end of the maxilla. Due to displacement, its exact contact relationships with other bones remain uncertain, but it is possible that it contacts the palatine anteriorly.

Palatine— In lateral view, the palatine is a rod-like bone whose caudal end extends laterally, forming a pyramidal boss ~~that is possibly the~~ point of articulation for the pterygoid. Laterally, the palatine is overlapped by the lacrimal and the maxilla, which is only observable through the

antorbital fossa. Due to overlapping and mediolateral compression, the overall morphology of the palatine and its contact relationships with other adjacent bones remains uncertain.

Laterosphenoid(?)— In lateral view, a small, laterally extending, pyramidal boss lies anteroventrally to the orbital process of the postorbital. Based on its relative location, it is highly possible that it could be part of the braincase and is interpreted as the laterosphenoid. This boss is similar to the lateral articular head of the laterosphenoid that would articulate with a socket on ventral margin of the frontal. However, due to poor preservation and overlapping, the true identification of this element, its morphology, and its ~~interrelationships~~ with other bones remain unknown.

Basioccipital—The basioccipital of IVPP V30936 disarticulated from the supraoccipital and is preserved upside down relative to ~~its position during life along with the basisphenoid.~~ Anteroventrally, the basioccipital contacts the basisphenoid but the suture between the two elements is ambiguous. In lateral view, the basioccipital is an inverted saddle-shaped element, as ~~is the case~~ in many neornithischians (Berta 2021; Jin et al. 2010; Peng 1992; Scheetz 1999). The basioccipital lies anterodorsal to the axis and caudoventral to the parietal, with ~~its~~ anteroventral margin overlapped by the atlas and its anterodorsal margin. The caudal end of the basioccipital narrows dorsoventrally to form the occipital condyle, which is posteriorly oriented, projects slightly ventrally with its anterior region becoming dorsoventrally longer with its lateral surface concave, and it forms the caudal part of basal tubera.

Basisphenoid—As described above, the basisphenoid is preserved upside down and the suture between the posterior basisphenoid and anterior basioccipital is ambiguous. The overall length of the basisphenoid is subequal to the length of the basioccipital. ~~The main body of the basisphenoid is visible in the lateral view and has the shape of an anterodorsally oriented cubic that forms the rostral part of the basal tubera~~. Its rostral region tapers ~~in width~~ to support the bifurcated basipterygoid processes, which are broken away but are visible ventrally. Both basipterygoid processes are anteroventrally oriented and blunt-ended, a plesiomorphy in neornithischians (Berta 2021; Peng 1992; Scheetz 1999). The angle between the two basipterygoid processes and the main body is approximately 35° degrees.

Supraoccipital— In lateral view, the supraoccipital is a rod-like bone posterior to the parietal. Due to compression, there is little information about its morphological characters and contact relationships.

Exoccipital— Only the left exoccipital is visible in lateral view. It is preserved upside down with its paraoccipital process broken away. Posteriorly, the exoccipital contacts the occipital condyle~~.~~ ~~It forms~~ the dorsolateral region of the magnum foramen. ~~It~~ is a roughly a cubic bone with a ~~process on its anterodorsal corner~~ extending laterally to form the paraoccipital process and medially to form a curve. On its caudodorsal corner, the exoccipital extends moderately laterally. The paraoccipital process is short and blunt.

Predentary— The left predentary is in close articulation with the dentary and is only visible in lateral view as a mediolaterally and anteroposteriorly compressed element. In lateral view, the

predentary is triangular with a short ventral process. The anteroposterior length of the predentary is extremely short at approximately half the anteroposterior length of the premaxilla, which is a plesiomorphy in neornithischians (Butler 2008) . The dorsal margin of the predentary is much longer than the ventral margin. The rostral tip does not project above the main body, similar to *Haya* (Berta 2021) and *Changchunsaurus* (Jin et al. 2010); ~~a plesiomorphy in neornithischians~~. The ventral process is much shorter than lateral process.

Dentary—Both dentaries are preserved and observable. The left is visible in ~~the~~ lateral view and the right is observable in medial view. Because the postdentary elements are displaced, the exact relationships with the dentary and other elements are uncertain. The dentary is an elongated and dorsoventrally thin element with a prominent, posterodorsally oriented process on the caudal end that contributes to the coronoid process. The dorsal margin and the ventral margin of the dentary are subparallel to each other along most of the length with the dorsal margin being greater. Both margins converge rostrally to form the articulate surface for the predentary, which is dorsally adjacent to the ventral margin, a synapomorphy also observed in *Changchunsaurus* (Jin et al. 2010). The lateral side of the dentary is smooth and unornamented. Four nutrient foramina are present on the lateral side and are ~~moderately ventral to~~ the dorsal margin of the dentary (FIGURE 2）. The caudoventral region of the dentary is concave and forms the point of articulation for the surangular and the angular. The dentary reaches its maximal height on its caudal margin, forming a caudodorsally projecting process that contributes to the coronoid ~~eminence.~~ The medial side of the dentary is relatively flat mediolaterally when compared to the lateral side. The Meckelian sulcus is located near the ventral margin along the medial surface of

the dentary. The posteroventral margin of medial dentary surface is covered by the plate-like splenial.

The dentary tooth row is medially inset to form the buccal emargination, similar to the maxillary tooth row. Because the dentary tooth row is obscured by the maxillary tooth row, the exact number of dentary teeth is unknown. Only six dentary teeth are visible in total between the rostral and caudal ends of the left dentary. The shape of dentary teeth resembles the maxillary teeth. The first small dentary tooth is adjacent to the predentary, similar to many early-diverging neornithischians(Norman et al. 2004; Sereno 1991; He et al. 1984).

Splenial—Both splenials are preserved although ~~there exists a long break on the dorsal border of the right element that has resulted in its anteroventral end being lost~~. ~~However,~~ most of the left splenial is overlapped by the dentary, though the right one is observable in medial view. Although their exact contacting relationships with other bones are ambiguous due to displacement, ~~enough is preserved to demonstrate that they~~ cover the caudoventral margins of the dentary's medial margins. The splenial is ~~generally~~ a subtriangular sheet. Its caudal end bifurcates into a blunt dorsal process and an elongate, tapering caudoventral process. From anterior to ~~caudal,~~ its dorsoventral length thickens. Its anteroventral end is broken and lost, so it ~~couldn't be~~ determined whether there exists a foramen on the rostral end.

Surangular—The left surangular is displaced and preserved upside down, exposing its medial side. It is a roughly flat, subtriangular element composed of three processes in medial view with no observable foramina along its surface. There are no foramina ~~observed in~~ other ornithischians such as *Haya* (Berta 2021), *Thescelosaurus* (Boyd 2014), *Changchunsaurus* (Jin et al. 2010); a

trait that is considered a synapomorphy that is commonly observed in early-diverging neornithischians. Due to displacement, the exact contacting relationships with other elements remain uncertain. The anterodorsal process is an elongate, arched, and slender process that possibly contacts the angular ventrally. At its base, the medial process of the surangular is flat. The anteroventral process is short and blunt-ended. The elongated, posterior-oriented process on the caudoventral corner is the retroarticular process, whose caudal end becomes concave to contact the articular.

Articular— The articular is ~~roughly a trapezoid or cubic~~ element when viewed laterally. It is disarticulated from the retroarticular process and the quadrate, ~~so~~ its specific relationships with other elements ~~is~~ unknown. ~~Its~~ ventral border extends laterally to form a ridge.

Angular— The left angular is visible in medial view where it forms the caudoventral border of the mandible. ~~In medial view, it~~ is subrectangular. As with other cranial elements, its exact contact relationships with other elements remain uncertain due to taphonomic displacement. On its anterior border, the angular is mediolaterally concave. On the posterior border, it is mediolaterally convex, forming the possible articulating surface for the surangular.

Hyolaryngeal apparatus— A pair of elongate, flat, leaf-shape ~~elements~~ that are L-shaped cross-section are located ventral to the mandible. The length of the arytenoids is about 80% of the dentary length. This pair of elements is similar to ossified arytenoids observed in *Pinacosaurus* (IGM100/3186) (Yoshida et al. 2023). Each arytenoid is composed of a mediodorsal wing and a dorsolateral wing（FIGURE 3）. The mediodorsal wing projects mediodorsally to form the arytenoid process which serves as an attachment site for the *M. dilator* (Yoshida et al. 2023). The

dorsolateral wing widens posteriorly before tapering at the caudal end. The lateral edge, especially at its rostral end, is rugose, which is the possible articulation ~~place between the arytenoids and the~~ cricoid.

A pair of elongated, gracile rod-shaped elements – which are interpreted here to be the ceratobranchials – are overlapped by the arytenoids and meet at a point that is posteroventral to the mandible. The length of ceratobranchials is less than 40% of the dentary length.

Postcranial elements

Cervical series（FIGURE 4）— A mostly complete cervical series is preserved in the specimen. Due to deformation and obscured elements, the exact number of cervical vertebrae is unknown. However, ~~there could be~~ nine cervical preserved in the specimen, since nine cervical vertebrae usually occur in early-diverging ornithopods (Han 2012), while fewer occur in Thyreophora and more than nine cervical vertebrae appear in later-diverging ornithopods and ceratopsians (Han 2012). The first three cervical vertebrae are visible in the lateral view. The following vertebrae are observable in the dorsal view, though they are majorly deformed and obscured. The 8th and 9th cervical vertebrae are disarticulated from the rest of the series. Most of the cervical ribs are disarticulated and scattered with the exception of the 5th and 6th cervical ribs. The sutures of the axis and 3rd cervical vertebra between the cervical neural arches and centra are unfused.

The atlas（FIGURE 2, 4） is visible in left lateral view. The proatlas and the atlantal ribs are not preserved. The atlantal intercentrum is disarticulated from the neural arches and is visible in anteroventral view ventral to the axis. In ventral view, the atlantal intercentrum is subcrescentic in shape. The anterior side of the atlas is excavated by a fossa that is the deepest on the midline and becomes shallower laterally. The lateral margins of the atlas expand

dorsoventrally to form the transverse processes. A flange extends on the ventral margin that demarcates the anterior side of the atlas from the ventral side. A groove is located along the ventral side of the atlas, ~~which is a synapomorphy also observed~~ in *Jeholosaurus* (Han 2012) and *Hexinlusaurus* (He et al. 1984). In lateral view, the neural arches are a pair of wing-shape elements expanding dorsolaterally which are jointed at the base. The transverse width of the base narrows from rostral to caudal. The base has two articulating surfaces, a posterodorsal one for the odontoid process and a ventral one for the intercentrum. The pleurocentrum of the atlas becomes the odontoid process fused to the axis. The odontoid process is taphonomically compressed. The prezygapophysis is not visible while the postzygapophysis is developed to articulate with the prezygapophysis of the axis.

The axis（FIGURE 2, 4） is well-preserved, is observable in lateral view, and is comprised of the intercentrum, the centrum and the neural arch. The neural spine is a dorsoposteriorly oriented crest. Its relative anteroposterior length is not as long as those of many ornithischians in which it extends beyond the posterior margin of the 3rd cervical (Berta 2021; Han 2012; Butler et al. 2011), a plesiomorphy in neornithischians). At the base of the neural spine, ~~there exists an obvious~~ prezygapophysis on the rostral end and a well-developed postzygapophysis on the caudal end that articulates with the prezygapophysis of the third cervical. A round ~~diaphysis~~ is located ventral to the prezygapophysis on the anterolateral surface of the neural arch. The height of the neural arch is subequal to that of the centrum. The suture between the neural arch and the centrum is not fused. The centrum is opisthocoelous. The ~~paraphysis~~ is a small process present on the anterodorsal surface of the centrum. A wedge-shaped intercentrum is anterior to the centrum. The axial rib is disarticulated and missing. Based on the presence of both the diaphysis and the paraphysis, the axial rib is likely double-head.

559 The third cervical (FIGURE 4) is observable in lateral view though its caudal region is broken
560 due to preservation. ~~Its~~ overall shape and composition are similar to that of the axis except it
561 lacks an intercentrum. Compared to the axis, ~~its~~ neural spine is much smaller and more
562 posteriorly oriented. The prezygopaphysis is better developed and its diaphysis is smaller and
563 more posteroventrally located. The paraphysis is larger than the axis.
564 The following cervical series (FIGURE 4) are visible in dorsal view but are majorly damaged
565 and obscured. Their anteroposterior length is longer than their transverse width. The 4th cervical
566 vertebra is composed of a pair of visible, well-developed, lateroposteriorly oriented transverse
567 processes, well-developed postzygapophyses, and a small, dorsoposteriorly oriented neural arch.
568 The possible two-head rib of the 4th cervical vertebra is ventral to the transverse process. The
569 5th cervical vertebra is comprised of a pair of well-developed prezygapophyses, a
570 lateroposteriorly oriented transverse process that articulates with a double-headed rib, and a
571 small, dorsoposteriorly oriented neural arch. The 6th cervical vertebra is comprised of a small,
572 dorsoposteriorly oriented neural arch, and a lateroposteriorly oriented transverse process that
573 articulates with a double-headed rib with more than twice the anteroposterior length of the
574 centrum of the 6th cervical vertebra. The 7th, 8th and 9th cervical vertebrae are so compressed
575 that little morphological information can be meaningfully extracted from them.
576
577 Dorsal vertebrae and dorsal ribs (FIGURE 5)— Most dorsal vertebrae are obscured, deformed,
578 or overlapped by the ribs and ossified tendons. Only three posterior dorsal vertebrae close to the
579 ilium can be fully observed in lateral view. The dorsal vertebrae are *amphiplatyan or* moderately
580 *procoelous. Only one* obvious diapophysis is visible (FIGURE 5). There is no unambiguous
581 evidence of striated rims around the anterolateral and posterolateral borders of the centra. Most

582 dorsal ribs are obscured or disarticulated, and all are compressed. Six recognizable double-head
583 and moderately bowed dorsal ribs are articulated with anterior dorsal vertebrae (FIGURE 5).
584 There is no evidence of the existence of intercostal processes.
585 Sacral vertebrae— All sacral vertebrae are overlapped by the ilium.
586
587 Caudal vertebrae— In lateral view, much of the caudal series of vertebrae is preserved. The
588 preserved caudal vertebrae include two vertebrae (FIGURE 7 A), 5 middle vertebrae (FIGURE 7
589 B), and seventeen posterior vertebrae (FIGURE 7 C). Most anterior caudals are damaged or
590 missing while most of the posterior vertebrae are missing. All preserved caudal vertebrae are
591 amphiplatyan. The anteroposterior length gradually increases while the dorsoventral height
592 decreases. The neurocentral sutures of all caudal vertebrae are unfused.
593 The centra of the anterior caudals are dorsoventrally concave. The ratio between
594 anteroposterior length and dorsoventral length of the vertebrae is close to 1.5. Their neural arches
595 are low on the centrum and all neurocentral sutures are obvious. ~~The~~ prezygapophyses and
596 postzygapophyses ~~both~~ extend a little beyond the anterior and posterior margins of the centrum,
597 respectively. The hatchet-shaped neural spines are flat and more elongate than those of the
598 posterior caudals, are positioned moderately anterior to the postzygapophyses extending
599 posterodorsally, and are dorsoventrally expanded. The chevrons are disarticulated and are an
600 elongated rod-shape in lateral view.
601 Middle caudals are similar to anterior ones except that the dorsoventral length of the middle
602 caudal centrum is narrower than that of anterior ones. Small transverse processes are present at
603 the base of the neural arches. In the lateral view, there are two hatchet-shaped chevrons
604 disarticulated with the centrum.

From proximalmost vertebra to the distalmost, the dorsoventral length of the posterior caudal vertebrae decreases and the anteroposterior length increases to be more than twice the dorsoventral length. The prezygapophyses extend beyond the anterior end of the centrum. Unlike the middle caudals, the postzygapophyses do not extend beyond the posterior end. The former articulates with the latter. From anterior to posterior, the anteroposterior length of the prezygapophyses and postzygapophyses gradually increases, the dorsoventral lengths decrease and both are fused into a single unified structure. There are fourteen chevrons of the posterior caudal vertebrae preserved, twelve of which are articulated with the anteroventral corner of the centrum whose orientations gradually shift from vertical to horizontal. In lateral view, the chevrons are flat and hatchet-shaped while in anterior view they are 'Y'-shaped with two gracile proximal processes merging into one ventrally oriented tapering process.

Ossified tendons (FIGURE 7)— Ossified tendons are present along ~~with~~ the vertebral column. They are found alongside the middle dorsal vertebrae and the sacral vertebrae but are absent from the caudal vertebrae; a plesiomorphy among neornithischians (Berta 2021; Han 2012; Peng 1992; He et al. 1984). In lateral view, the ossified tendons are preserved as compressed, black filaments that are arranged in ~~the~~ basket-like arrangement~~s~~ of fusiform tendons along the caudal region. They lack a lattice arrangement and are more similar to a linear bundle arrangement.

Scapula（FIGURE 7）— Both scapulae are heavily damaged and compressed. Only part of the proximal plate of the right scapula, and fragments of the proximal and distal ends of the left scapula are observable in lateral view. As a result, the exact shape of either scapula remains unknown; however, it could be determined that the scapula formed an elongate and strap-like

shape. Similar to most small ornithischians, but different from *Koreanosaurus* (Min et al. 2011) and *Oryctodromeus* (Krumenacker 2017), the scapula is unfused with the coracoid; a plesiomorphy in neornithischians. The acromion, positioned at the anterodorsal corner of proximal plate, is relatively blunt as it is not prominent and does not develop into the scapular spine. Both the dorsal margin and the ventral margin of the proximal end of the scapula are concave. A laterally concave fragment of the distal end is located far from the proximal plate. Although the overall shape of the distal end of the scapula is unknown due to damage, the fragmentary remains possibly suggest that the dorsoventral width of the scapula gradually decreases posteriorly.

Coracoid（FIGURE 7）— Both coracoids are preserved but displaced. The description below about orientation is based on the fully exposed right coracoid. In lateral or medial view, the coracoid is a smooth, subquadrate plate with a concave medial surface. The dorsoventral length is subequal to the anteroposterior length. Its ventral border is relatively straight while the dorsal border is strongly concave to form an embayment observed in many other species (Berta 2021; Min et al. 2011; He et al. 1984; Yang et al. 2020). The posterior border which is sutured with a scapula is smooth while the anterior one is much more rugose. No foramen, also observed in *Haya* (Daniel E. Berta 2021), *Hexinlusaurus* (He et al. 1984), *Jeholosaurus* (Han 2012) , and many other taxa, is present, which is an autapomorphy for *Pulaosaurus*.

Sternum（FIGURE 7）— Only a proximal fragment of the left sternum is preserved. The degree of fracturing to the sternal elements has made the total shape unknown. The proximal fragment is mediolaterally thin. This fragment is fan-shaped along its proximal end and is

651 dorsoventrally broad but gradually narrows from anterior to posterior, so it is likely that the
652 sternum is a hatchet-shaped or a shafted element. No parascapular spine is observed.
653
654 Humerus（FIGURE 8）— Only the left humerus is preserved completely with its head partially
655 overlapped by the coracoid. The left humerus is visible in anterior view. Generally, the humerus
656 is similar to many small early-diverging neornithischians ~~in that it is~~ a relatively gracile element
657 compared to the humerus of *Koreanosaurus* (Min et al. 2011), *Tenontosaurus* (Winkler & Murry
658 1997). The gracile form of the humerus is a plesiomorphy for neornithischians. The length of the
659 humerus is about half the length of the femur. ~~Its~~ anteroposteriorly thin proximal end expands
660 mediolaterally to form the head, which is rotated 37° relative to the shaft. The anterior surface
661 of the head has a concave shape that forms the bicipital sulcus. The deltopectoral crest is
662 damaged, so its ~~total~~ shape is unknown. The lateral tuberosity is obscured by the coracoid while
663 the medial tuberosity is continuous with a ridge defining the proximal end concavity. The shaft is
664 gracile and short with an elliptical cross-section. An intercondylar groove extends along the shaft
665 to form an oval intercondylar fossa near the distal end of the humerus. The ulnar condyle is
666 larger than the radial condyle and extends ~~anteriorly and distally~~.
667
668 Ulna and radius (FIGURE 8)— The right and left ulnae, and right and left radii are all preserved
669 in anterior view. Both ulnae and radii are straight, rod-like elements ~~with~~ both ~~being~~ shorter than
670 the humerus. The proximal end of the ulna is broad, and the shaft narrows distally with the distal
671 end moderately expanded. ~~Its~~ olecranon process is low, which is a plesiomorphy usually
672 observed in early-diverging neornithischians (Peng 1992; He et al. 1984). ~~Its~~ medial coronoid
673 process makes the medial border keeled, as in *Orodromeus* (Scheetz 1999), *Changmiania* (Yang

et al. 2020) and *Koreanosaurus* (Min et al. 2011). ~~On~~ the cranial surface of proximal humerus, ~~there exists~~ concave, triangular articular facet for articulation with the radius. On the cranial surface of the distal end, there also exists a similar triangular, concave surface to articulate with the distal end of the radius except that it is smaller and shallower. Compared to the ulna, the radius is slender and gracile.

Carpals (FIGURE 8)— The left carpals are well-preserved and in articulation while the right carpals are preserved disarticulated with each other. ~~Due to this, the description below is based on the left carpals~~. The carpals are composed of ulnare, radiale, intermedium, and one distal carpal ~~with all being visible~~ in dorsal view. The ulnare is a cranially convex, pyramidally-shaped block that articulates distally with the ulna. The intermedium is located medial to the ulnare and is a square block with a proximally convex margin that distally articulates with the ulna. Compared to the ulnare, the radiale is similar in shape ~~and articulation with the ulna but is smaller in size~~. The distal carpal is pentagonal in outline, dorsally convex, and articulates with the third metacarpal ventrally.

Metacarpal (FIGURE 8)—All five of the left metacarpals are preserved in relative articulation while the right metacarpals are preserved but disarticulated with each other. The description ~~below~~ is based on the left metacarpals. Metacarpal 1 is compressed ~~with~~ metacarpals 2-5 being well-preserved. ~~All metacarpals are observable in~~ posterior ~~view.~~ The second metacarpal is the longest, followed by the third and the fourth. The fifth is the shortest and is almost perpendicular to the others. The proximal ends of the metacarpals are blunt and expanded. The shafts are constricted with the shaft of metacarpal 3 being constricted most abruptly. The distal ends of the

metacarpals are moderately expanded with ginglymoid articulations. On the distal ends, the lateral condyles are larger than the medial condyles, making the metacarpals medially oriented. A shallow, oval fossa exists between the distal condyles.

Carpal phalanges (FIGURE 8)—The left carpal phalanges are preserved relatively in articulation while the right metacarpals are preserved disarticulated with each other. ~~Due to this, the~~ description ~~below~~ is based on the left carpal phalanges. The carpal phalanges are observable in posterior view. The phalangeal formula is 2-3-4-3-2. The proximal-most phalange of the digit 2 is the longest. ~~The phalanges except for the unguals~~ have ginglymoid articulations with each other ~~articulated.~~ The unguals of manual digits 2 and 3 are claw-like, the unguals of manual digit 1 are subconical while the unguals of manual digits 4 and 5 are blunt.

Ilium (FIGURE 9)— Only the right ilium is visible in IVPP V30936, which is preserved upside down. The ilium is composed of an elongate and tapering preacetabular process, the main body, and a dorsoventrally deep, anteroposteriorly short postacetabular process. The ischial peduncle is also compressed and damaged, so the exact shape of the ischial peduncle is unknown. As it is also disarticulated with pubis and ischium, it is unknown whether the acetabulum is closed or not. Similar to *Dryosaurus* (Galton 1981), the preacetabular process is elongate, dorsoventrally narrow, and tapering. The preacetabular process is longer than the postacetabular process. The shape of the dorsal border is uncertain as it may be deformed. The acetabulum is anteroposteriorly long and dorsoventrally narrow. On the anterodorsal corner of the acetabulum, there is a supraacetabular crest that extends moderately laterally, which is a synapomorphy only seen in early-diverging ornithischians including *Agilisaurus* (Peng 1992) and *Eocursor* (Butler 2010) but absent in Heterodontosauridae(Butler 2010). The pubic peduncle is anteroventrally

oriented and tapers into a stout and subrectangular process in lateral view. The ischial peduncle is also anteroventrally oriented with a suboval articulate surface. Dorsoposterior to the ischiac peduncle, a suboval and shallow brevis fossa is present.

Ischium (FIGURE 9)— The left ischium is preserved with its proximal end overlapped by a rib and the left femur ~~with its~~ distal end overlapped by the left tibia. The ischium is a rod-like element that contacts the pubis anteroventrally. The proximal end is divided into the pubic peduncle and the iliac peduncle. In lateral view, the pubic peduncle is anterodorsally oriented while the iliac peduncle is posterodorsally oriented. The former is anteroposteriorly broader and longer than the latter. The concavity between both is dorsoventrally shallow and anteroposteriorly broad. The obturator process is small and subrectangular. Similar to *Gilmoreosaurus mongoliensis* ~~ischium~~ (AMNH FARB 30739) (Prieto-Márquez & Norell 2010), this concavity is located very close to the pubic peduncle and forms the obturator foramen with the pubis, which is a synapomorphy of *Pulaosaurus*. The shaft is ~~in posteroventral orientation with its distal end weakly expanded.~~

Pubis (FIGURE 9)— The left pubis is preserved with its proximal end overlapped by the right femur. It is a slender, mediolaterally thin, rod-like bone in posteroventral orientation. The length of the pubis is subequal to the left ischium. ~~It~~ contacts the left ischium on the dorsal border of the shaft. Compared to the ischium, the pubic body is smaller ~~than the ischium~~. Due to overlapping, the prepubic process is not visible. The obturator opening in the pubis is a notch-shape and forms the obturator foramen with the pubis, which is a synapomorphy of early-diverging neornithischians - as observed in *Haya* (Berta 2021), *Jeholosaurus* (Han 2012), and *Thescelosaurus* (Brown 2011).

743

744 Femur (FIGURE 11)— Both femora are preserved in medial view. The distal end of the left
745 femur is broken while the right femur is compressed with its fourth trochanter broken. The femur
746 is robust with an elliptical cross-section and is longer than the humerus. The femoral head is
747 perpendicular to the shaft which is bowed anteriorly. The neck between the head and the shaft is
748 not visible. The fourth trochanter is pendant-shaped and is moderately proximal to the midlength
749 of the shaft. Although the distal end is broken, eroded, or compressed, the medial condyle of the
750 distal end is larger than the lateral condyle based on the morphology of the intercondylar groove.
751 However, due to incomplete or deformed preservation of the distal end, the exact shape of the
752 intercondylar fossa is unknown.

753

754 Tibia (FIGURE 11)— Both tibiae are preserved. The left tibia is observable in anterior view
755 while the right tibia is observable in medial view. Tibiae are elongate, rod-like bones. The tibia is
756 moderately longer than the femur with the ratio between the left tibia and the left femur being
757 1.10 while the ratio between the right tibia and femur being 1.22. Both ratios are typical of most
758 early-diverging neornithischians (Berta 2021). Due to displacement of the left fibula and tarsals,
759 the ~~left tibia distal end~~ overlapped by the fibula, thus obscuring the ~~exact contacting relationship~~
760 between the left tibia and the left fibula. In anterior view, the proximal end of the tibia extends
761 anteriorly. The cnemial crest develops poorly to form a short, anterolaterally extending ridge that
762 is separated from the fibula condyle by the deep incisura tibialis. In anterior view, the fibula
763 condyle is prominent and broader than the cnemial crest and extends anteriorly and proximally.
764 A tiny accessory condyle lies medial to the fibula condyle. The shaft of the tibia is elongated,
765 and the cross-section is elliptical in shape. The shaft expands moderately laterally to form a

laterally convex ridge, the fibula eminence, to contact the fibula. In medial view, the distal end of the tibia expands anteroposteriorly and in anterior view it expands mediolaterally to form the internal malleolus and the external malleolus. A shallow groove separates the internal malleolus and the external malleolus. The external malleolus is obscured by the distal end of the left fibula. The medial malleolus is salient medially and extends anteriorly.

Fibula (FIGURE 11)— Both fibulae are preserved, but only the left one is observable in anterior view. It lies lateral to, and unfused with, the left tibia. However, due to its displacement, its exact contact relationship with the tibia is unknown. Compared to the left tibia, the length is subequal to the length of the tibia while it is much more gracile. In anterior view, the proximal end of the fibula is narrow and extends anteromedially. The shaft is bowed laterally. From its midpoint to the distal third of the fibula, it narrows to form an anteriorly extending flange. The distal end of the fibula gradually expands mediolaterally.

Astragalus and calcaneum (seen in FIGURE 12)—Astragali and calcanea of the right hindlimb are both preserved. In anteroventral view, the right astragalus and calcaneum contact the distal end of the right tibia proximally and are tightly appressed to each other ~~closely~~ without ~~being fused together~~. The left astragalus is displaced, but it is visible in dorsal view. The astragalus and calcaneum are not fused to the distal end of tibia, similar to the condition seen in *Hypsilophodon*(Huxley 1870), *Orodromeus* (Scheetz 1999), *Haya* (Berta 2021), *Changchunsaurus* (Butler et al. 2011), *Jeholosaurus* (Han 2012) and *Oryctodromeus* (Krumenacker 2017).

The astragalus is sub-rectangular in dorsal view and subtriangular in anterior and posterior views. Only the dorsally extending anterior face and the concave dorsal astragalus surfaces are visible. The anterior face of the astragalus forms the ascending process, which is represented as a subtriangular flange that extends dorsolaterally. This character is a synapomorphy for *Pulaosaurus* and *Gilmoreosaurus mongoliensis* (Ruiz-Omeñaca et al. 2012). ~~Its~~ lateral margin curves are moderately anteroposteriorly longer than the medial margin. ~~On the lateral margin, at the base of the ascending process, there exists a small oval articulating surface for the distal end of the fibula~~. The medial margin of the dorsal surface is moderately convex to contact the calcaneum while the lateral margin is concave. The dorsal surface is dorsoventrally concave to form an elliptical fossa to articulate with the tibia.

The calcaneum is square in the anterior view. Due to preservation, little information about it is available.

Distal tarsals (FIGURE 12)— There are three distal tarsals preserved, which is the same number observed in *Heterodontosaurus* (Han 2012). This is possibly an ornithischian plesiomorphy (Norman et al. 2011; Peng 1992). Both left and right distal tarsal 1 are preserved. The left distal tarsals 2 and 3 are preserved. Distal tarsal 1 is situated above metatarsal 1 and 2, distal tarsal 2 is situated above metatarsal 3 and 4, distal tarsal 3 is situated above metatarsal 4, metatarsal 5 is dorsolaterally adjacent to distal tarsal 3. Distal tarsal 1 is a wedge-shaped element with a with a shallow fossa on its anterior surface. In posterodorsal view, an L-shaped element with a concave posterior surface. In posterodorsal view, it is a hinge-shaped element with a concave posterior surface. The dorsoventral height of distal tarsal 1 narrows from medial to lateral. In the anterior view, distal tarsal 2 is a block-like element, the mediolateral width of which is much longer than

its dorsoventral length. In the posterior view, distal tarsal 3 is a drop-shape element, the mediolateral width of which narrows from dorsal to ventral. A small foramen pierces the posterior surface of distal tarsal 3, a ~~synapomorphy~~ also observed in the posterior surface of distal tarsal 3 in *Jeholosaurus* (Han 2012).

Metatarsals (FIGURE 12)— The metatarsals are preserved as mostly complete elements. Right metatarsals I, II, III, and IV are visible in dorsal view while left metatarsals II, III, IV, and V are visible in ventral view. The proximal end of right metatarsal I is obscured by right metatarsal II. The midpoint and distal end of right metatarsal III are damaged and the distal half of right metatarsal IV is not preserved. Only the proximal end of metatarsal V is preserved as a small splint-like element that is dorsolaterally appressed to distal tarsal 3. Metatarsals are almost in the same plane and appressed to each other throughout most of their lengths. As in most early-diverging neornithischians, metatarsal III is the longest and the stoutest with its length being about twice the length of metatarsal I. Metatarsal I is splint-like with its proximal end mediolaterally compressed and its shaft gradually widening ~~from~~ proximodistally. In dorsal view, metatarsal II, III and IV are elongated, rod-like elements with the shafts proximodistally narrow and their distal ends moderately expanded. Shallow grooves, ginglymoid distal articular surfaces, and collateral ligament pits are present on the dorsal sides of distal ends. In the ventral view, medial condyles on the distal ends of metatarsal II, III and IV are larger than the lateral condyles.

Pedal phalanges (seen in FIGURE 12)— Right pedal phalanx I, II, III, IV, and left phalanx II, III, IV are preserved. Due to poor preservation, it is uncertain whether phalanx V exists in this taxon. Based on the preserved digits, the phalange formula of *Pulaosaurus* is 2-3-4-5-?, which is

similar to most early-diverging ornithopods and early-diverging ceratopsians (Norman et al. 2004; You & Dodson 2004). Most of the left digits are observable in the dorsal view except for the ungual digits of phalanx II and IV which are visible in ~~the~~ lateral view. Most of the right digits are observable in the ventral view except for the ungual digits of phalanx II, III, and IV which are visible in the lateral view, and phalanx I which is visible in the dorsal view. Right phalanx I and IV, and left phalanx III are disarticulated from their metatarsals. Except for ungual digits, the proximal and distal ends are expanded while the shafts are constricted. In dorsal view, except for III-1 and III-2, all of the left digits have dorsal lips on proximal ends that articulate with the extensor grooves of the preceding phalange distal ends. ~~On dorsal sides of III-1 and III-2, there exist deep oval collateral ligament pits on distal ends. On the ventral sides of the right phalanges,~~ lateral and medial condyles on distal ends are subequal. The intercondylar grooves are deep. All ungual digits preserved are claw-like.

Gut content（FIGURE 13）— On the posteroventral corner of the specimen's thoracic cavity, variegated impressions and flat peddles can be found. The shape of these impressions is not the same as each other and the diameter of these impressions ranges from 3mm to 8mm, obviously larger than the diameter of the surrounding matrix. The exact number of these impressions is unknown as it is hard to distinguish them from the surrounding matrix and their outlines are ambiguous. Different morphological characters and scattered distribution among these impressions make it impossible to be ovarian follicles as ovarian follicles that are preserved in fossil enantiornithine specimens are circular and uniform in size (Bailleul 2020; O'Connor et al. 2014; Wang et al. 2016). These oval or elliptical marks and flat peddles are similar to

impressions and cavities preserved in *Minmi* which are considered to be left by displaced plant seeds (Molnar 2000).

Therefore, it is possible that gut contents, like plant seeds, are preserved in this specimen. However, the actual identity of this thoracic anomaly needs further study that is beyond the scope of this project.

Discussion

Phylogenetic Analysis

The phylogenetic analysis of this study produced 19,701 most parsimonious trees of 1227 steps, a consistency index (CI) of 0.36, and a retention index (RI) of 0.71. The resolution of the strict consensus tree (FIGURE 14) is lower than the strict consensus tree by Han et al. (Han 2017). Most clades supported by the previous strict consensus tree by Han et al. (Han 2017), except for Pachycephalosauria, Iguanodontia, Neoceratopsia, Thyreophora, are not supported by this strict consensus tree. Most early-diverging ornithischian taxa and early-diverging neornithischian taxa form a polytomy which makes it difficult to recover the phylogenetic relationships between early-diverging ornithischian and early-diverging neornithischian taxa, especially the phylogenetic position of *Pulaosaurus*. This is possibly because of the incompleteness of morphological characters found in unstable taxa, as the results and resolution of different phylogenetic analyses also vary with the sampling taxa, the sampling characters and the completeness of specimens (Brown et al. 2022).

The reduced tree(~~seen in~~ FIGURE 15). is from 500 of the most parsimonious trees of 1195 steps, with a consistency index (CI) of 0.37 and a retention index (RI) of 0.71. The resolution of the reduced strict consensus tree is much higher compared to the strict consensus tree. It supports

most clades established by previous analyses(Han 2017). The reduced strict consensus tree recovers *Pulaosaurus* as one of the most early-diverging taxa of neornithischians ~~as~~ *Agilisaurus,* ~~more early-diverging than~~ *Hexinlusaurus*. This result agrees on the topology of previous analyses (Boyd 2015; Han 2017; Dieudonné et al. 2020; Butler 2008).

The monophyly of Neornithischia is supported by the combination of following synapomorphies: buccal emargination on the maxilla; both of the quadrate condyles are subequal in size; the frontal ~~doesn't~~ participate in the supratemporal fenestra; a longitudinal ridge is present along the basioccipital; a well-developed coronoid process is present on the mandible; the external mandible fenestra is absent; the prepubic process is rod-like or dorsoventrally compressed. The combination of following synapomorphies support the monophyly of Cerapoda: enamel distribution on cheek teeth is asymmetric; the number of sacral vertebrae increases from 4 or 5 to 6 or more; the ischial peduncle of the ilium projects ventralaterally; the fossa trochanteris modified into distinct constriction separates the head and the greater trochanter of the femur; the anterior trochanter of the femur is closely appressed to the greater trochanter; metatarsal I is robust and well-developed with the distal end of phalanx I-1 projecting beyond the distal end of metatarsal II. Based on these phylogenetic analysis results, as the anterior side of *Pulaosaurus* femur and the sacrum is not visible in this specimen, it is possible that *Pulaosaurus* could be a Cerapodan species.

The overall trend of characteristic evolution from early-diverging neornithischian taxa to later-diverging Ornithopoda taxa includes these changes: 1.the number of the premaxillary teeth decreases and the premaxillary teeth even become absent; 2. the contact between the posterolateral process of the premaxilla and the lacrimal changes from absent to present, excluding the jugal from the antorbital fossa; 3. the ventral margin of the premaxilla gets

deflected ventrally to maxillary tooth row and flares laterally; 4. the external naris extend posteriorly to lie above the maxilla and their ventral border rise; 5. the edentulous maxillary anterior margin length increases; 6. the antorbital becomes observable ~~and from~~ subtriangular to oval or subsquare, ~~its~~ position changes from partly below the orbit to entirely anterior to the orbit; 7. the suture between the maxilla and the jugal changes from scarf joint to 'finger-in-recess' joint;8. the ventral edge of the jugal curves more strongly posteroventrally; 9. the posterior process of the jugal changes from weakly expanded to either forked or strongly expanded and bluntly truncated and expands more towards the squamosal; 10. the postorbital projects more into the orbit and the length of the squamosal process increases;11. the free portion of the quadrate gets longer, the quadrate condyle articular surface changes from ventromedially inclined to either ventrolaterally or horizonal, the quadrate foramen changes from absent to present; the frontal gets longer and narrower;12. the depression on lateral surface on the squamosal continuous with the caudodorsal infratemporal fenestra extends more to above the quadrate head; 13. the contribution of supraoccipital to the dorsal margin of foramen magnum becomes less, its dorsal margin length increases, its ventral margin length decreases, its relative width decreases; 14. the basal tuber of the basisphenoid gets thicker anteroposteriorly, the orientation of the basipterygoid processes deflect more posteriorly, the basipterygoid process articular facet for the pterygoid gets bigger and decreases in relative dorsal length;15. the pterygoid mandibular process decreases in relative length; 16. the predentary gets longer and more pointed, ~~its~~ oral margin gets denticulate, ~~its~~ ventral process changes from single to bifurcated; 17.the diastema between the first dentary tooth and the predentary changes from absent to present and its length increases, the number of dentary teeth increases, the number of the maxillary teeth increases from less than 15 to more than 20, the shape of cheek teeth changes

from subtriangular to diamond-shaped, the shape of cheek tooth crown changes from triangular to rounded, the apicobasally extending ridges on the labial surface of the cheek teeth changes from absent to present and from not confluent with denticles to confluent with denticles, the primary ridge along cheek teeth gets more prominent, the maxillary tooth ridge gets more prominent than the dentary one, the crown height of cheek teeth increases, the anteroposterior width of maxillary crowns become narrower than dentary crowns, the shape of the marginal ornaments changes from serrations to denticles, the asymmetry of enamel distribution increased; 18.the level of the jaw joint becomes lower;19. the number of cervical vertebrae increases from 9 to more than 10, the length of cervical vertebrae decreases, their postzygapophyses get more arched;20. the number of dorsal vertebrae increases from 12 or 13 to more than 16, the height of dorsal vertebrae neural spine increases;21. the number of sacral vertebrae increases from 2 to more than 6, the length of anterior vertebrae transverse processes relative to neural spine height decreases; 22. proximal caudal neural spines increase in height; 23.the arrangement of ossified tendons change from longitudinally arranged to basket-like arrangement of fusiform tendons in caudal region; 24.the relative length of the humerus increases; 25.the shape of proximal carpals change from ovoid to block-shaped; 26. the articulation between carpals and metacarpal I changes from free to coossified; 27. the proximal ends of metacarpals become block-like, the relative length of metacarpal I and II decreases, the shape of metacarpal I changes from elongated to block-like; 28. the shape of manual digit I ungual changes from claw-shaped to subconical, the phalangeal number of manual digit III decreases from 4, the relative length of manual digits II–IV decreases, the ungual shape of manual digits II and III changes from claw-shaped to hoof-shaped, the relative length of phalanx 1 of manual digit V changes increases; 29.the dorsal margin of iliac blade changes from convex midsection to horizonal, the brevis and

fossa change from facing ventrolaterally and visible in lateral view to facing ventrally and not visible in lateral view, the eversion of dorsal margin of postacetabular process changes from absent or weak to prominent, the relative length of postacetabular process decreases, the supra-acetabular crest becomes absent; 30 the relative distance between the ischial process of the ischium and the pubic peduncle decreases; 31. the length of the pubis shaft decreases, the anterior pubic blade expands, the prepubic process changes from rod-like to either dorsoventrally or mediolaterally compressed, the angle between the prepubic process and the pubic shaft increases, the obturator foramen changes from a foramen to a notch; 32.the femoral shape in lateral view changes from bowed anteriorly along length to straight, the femora relative length increases, the anteroposterior length of the greater trochanter increases, the femoral ligament sulcus becomes more prominent, the anteroposterior length of the anterior trochanter decreases, the anterior trochanter gets more proximally to the femoral head, the fourth trochanter gets more distal to the head, the anterior intercondylar groove on distal end of femur changes from absent to present, the medial condyle on the posterior intercondylar groove of the femur gets inflated laterally; 33. the astragalar ascending process changes to subtriangular flange; the medial distal tarsal changes from articulating metatarsals II and III to only metatarsal II; 34.the relative length of pedal phalanges decreases, the pedal digit I goes absent.

Compared to later-diverging neornithischians, many plesiomorphies of Neornithischia are maintained in *Pulaosaurus*: the first maxillary tooth is close to the posterior margin of the premaxilla; the maxillary teeth are subtriangular without ridges; the forelimbs are relatively shorter; there are five digits on the manus; a supra-acetabular crest is located on the ilium; and there are three distal tarsals. ~~The above listed plesiomorphies suggest~~ *Pulaosaurus* is one of the earliest-diverging neornithischians. However, there are also derived synapomorphies also present

971 in *Pulaosaurus*. For example, the squamosal forms a glenoid to articulate with the quadrate, a
972 ceratopsian synapomorphy, is present in *Pulaosaurus*; the posterolateral process of the
973 *Pulaosaurus* premaxilla contacts the lacrimal, which is a synapomorphy of iguanodontian taxa
974 such as *Dryosaurus*, *Iguanodon*, and *Ouranosaurus*; the frontals of *Pulaosaurus* are elongated
975 and narrow which is more similar to early-diverging Ornithopoda taxa; the dorsal surface of the
976 squamosal is flat and expands laterally, a synapomorphy of Pachycephalosauria and certain
977 early-diverging ceratopsians such as *Yinlong* and *Huayangceratops*(You & Dodson 2004). This
978 all suggests that mosaic evolution has occurred in the evolution of neornithischians and some
979 synapomorphies of later-diverging neornithischian taxa have appeared early in basal taxa.
980 However, it should be noted that the results described herein are unstable due to the
981 incompleteness of specimens and the lack of certain morphological characteristics. To solve the
982 problems about early-diverging neornithischian phylogeny and recover the actual systematical
983 position of *Pulaosaurus*, more specimens and more complete fossil materials are required in
984 future research.
985
986 New information of distribution of early-diverging neornithischian taxa
987 Taxa of early-diverging Neornithischia in China are mainly found in the Middle Jurassic strata
988 in southwestern China: *Agilisaurus* (Peng 1992), *Hexinlusaurus* (Barrett et al. 2005),
989 *Yandusaurus* (He et al. 1984) are found in Lower Shaximiao Formation of Province Sichuan and
990 *Sanxiasaurus* (Li et al. 2019) are found in Xintiangou Formation of Chongqing. *Agilisaurus* and
991 *Hexinlusaurus* are considered as the most early-diverging neornithischian taxa by most analyses
992 (Boyd 2015; Dieudonné et al. 2020; Butler 2008) while *Sanxiasaurus* is the earliest record of
993 Neornithischia in Asia (Li et al. 2019). Fossil record of Neornithischia in northern China is
994 limited, including *Jeholosaurus* (Han 2012) and *Changmiania* (Yang et al. 2020) found in

Province Liaoning, *Changchunsaurus* (Jin et al. 2010) found in Province Jilin. ~~These neornithischian taxa are found in Lower Cretaceous strata of northern China (Yang et al. 2020; Liyong Jin et al. 2010; Han 2012).~~ There is a temporal and geographical gap among the distribution of early-diverging Neornithischia in China. Moreover, ~~as described in the introduction,~~ ornithischian taxa present in Jurassic fauna including the Shishugou and Shaximiao faunas are ~~of lack~~ in the Yanliao Biota (Liu 2022), which usually play the role of small and middle bodied herbivores in the ecosystem.

The finding of *Pulaosaurus* fills the temporal and geographic gap of neornithischian fossil record in China, providing new information on the biodiversity of the Yanliao Biota. Diyin Huang proposed that there was geographical isolation between northeastern China and other regions during the Middle and Late Jurassic, which inhibited the input of animals from other faunas and made the species composition of the Yanliao Biota different from other Jurassic faunas (Liu 2022). However, the finding of new neornithischian species in Upper Jurassic Tiaojishan Formation also suggests that Asian neornithischian taxa originating from the Middle Jurassic Sichuan Basin spread to northern China in the Late Jurassic and the Early Cretaceous, indicating that the geographical isolation of the Yanliao Biota ~~isn't too~~ strict to prevent the spread of vertebrates from other regions and there could be large-bodied vertebrates that ~~haven't~~ been found in the Yanliao Biota.

Hyolaryngeal apparatus and acoustic function of *Pulaosaurus*

The hyolaryngeal apparatus of Archosauria comprises the following elements: one basihyal, a pair of ceratohyals, one pair of ceratobranchials, one pair of cricoids, and one pair of arytenoids. Additionally, one procricoid, one pair of epibranchials and one paraglossal are only present in Aves (Yoshida et al. 2023; Friedman et al. 2018; Hill et al. 2015). In extant reptiles,

the hyolaryngeal apparatus elements are cartilaginous with the exception of the ossified ceratobranchials (Yoshida et al. 2023). In extant Aves, the ceratobranchials, the epibranchials, and the larynx are ossified (Yoshida et al. 2023). The hyolaryngeal apparatus plays a significant role in acoustic function, airway protection, respiratory modification, and circulation assistance in tetrapods (Kirchner 1993). However, few fossilized larynx elements have been found in non-avian reptile fossils when compared to their significance in Archosauria evolution and ecology. In the case of the Dinosauria, most non-avian dinosaur specimens only preserve the first pair of rod-like ceratobranchials. Other hyolaryngeal elements preserved are ~~described below: in~~ *Carnotaurus*, *Microraptor, Confuciusornis*, the basihyal is found (Bonaparte et al. 1990; Yoshida et al. 2023); the basihyal and ceratohyals are preserved in *Saichania chulsanensis* (Bonaparte et al. 1990; Yoshida et al. 2023); a pair of ceratobranchials and the epihyal are preserved in *Pinacosaurus granger* (Morschhauser 2013); the plate-like second pair of ceratobranchials is preserved in *Psittacosaurus mongoliensis* (Morschhauser 2013); the splint-like second pair of ceratobranchials is preserved in *Leptoceratops gracilis* (Morschhauser 2013); the ~~tetraiadiate~~ first pair of ceratobranchials and the plate-like second pair of ceratobranchials are preserved in *Protoceratops andrewsi* (Morschhauser 2013); the sigmoid ceratohyal and the basihyal are preserved in *Triceratops horridus* (Morschhauser 2013). *Pinacosaurus granger* has been the first dinosaur whose larynx element has been reported (Yoshida et al. 2023). *Pulaosaurus* is reported as the second dinosaur specimen with larynx apparatus since *Pinacosaurus granger*, which demonstrates that an ossified hyolaryngeal apparatus ~~has~~ existed more broadly among non-avian dinosaurs and not just in ankylosaurids. *Pulaosaurus* also possesses a pair of rod-like ceratobranchials, which is also preserved in *Jeholosaurus* and many other dinosaur species (Friedman et al. 2018).

The arytenoids of *Pulaosaurus* are elongated with arytenoid processes, the length of which is about 80% of the dentary length. This structure is similar to the arytenoids preserved *Pinacosaurus*, but the arytenoid processes of *Pulaosaurus* are less prominent. In the case of acoustic function, the larynx functions differently between extant Aves and non-avian reptiles (Yoshida et al. 2023). In extant non-avian reptiles – such as turtles and crocodiles – the larynx functions as the vocal source (Yoshida et al. 2023; Sacchi et al. 2004; Riede et al. 2015). During phonation, the glottis is almost closed by the larynx and its surrounding muscles and ligaments and then air pressure forces the glottis open ~~to make~~ vocal folds vibrate and phonate, thus producing sounds (Yoshida et al. 2023; Sacchi et al. 2004; Riede et al. 2015). In extant Aves, the vocal source is the syrinx, which is located at the lower end of the trachea (Kingsley et al. 2018; Yoshida et al. 2023; Sober et al. 2019), which has also been found in the Mesozoic bird *Vegavis* (Clarke et al. 2016). The larynx serves as part of the vocal resonator tract to improve vocal efficiency and sounds are emitted through it, which requires control over the glottal opening (Kingsley et al. 2018; Yoshida et al. 2023; Sober et al. 2019). A longer arytenoid provides more attachment area for the dilator muscle, thus making its lever arm longer, which assists the arytenoid with the opening of the glottis (Yoshida et al. 2023). The arytenoids, with their prominent arytenoid processes and firm cricoid-arytenoid joints, allow for horizontal rotation of the arytenoid to open and close the glottis (Yoshida et al. 2023). Such structures allow extant birds to communicate with more complicated sounds in broader vocal ranges and with greater efficiency (Yoshida et al. 2023; Sober et al. 2019). Yunki proposed that the arytenoid length is positively correlated to the mandible width and there is a distinction in relative arytenoid size when compared to the mandible among species ~~whose larynx functions as the vocal source and whose larynx functions as a vocal modifier~~ (Yoshida et al. 2023). Due to the compression of the

Pulaosaurus mandible, the exact width of the *Pulaosaurus* mandible is unknown, so we cannot calculate the acoustic function of *Pulaosaurus*. However, based on the cranial morphology, the *Pulaosaurus* mandible width is less than 8cm, which is the length of its skull. Therefore, the mandible width is shorter than the mandible width of *Pinacosaurus,* which is 10cm (Hill et al. 2015). *Pulaosaurus* arytenoids are subequal to those of *Pinacosaurus* in length (Yoshida et al. 2023). Therefore, the relative arytenoid length of *Pulaosaurus* is larger than *Pinacosaurus*. *Pulaosaurus* is highly likely to possess a non-laryngeal vocal source similar to *Pinacosaurus* although the acoustic function is more primitive as its arytenoid processes are less prominent. Its larynx possibly functions to modulate and enhance sounds, thus allowing *Pulaosaurus* to communicate with more complicated sounds, similar to extant birds (Yoshida et al. 2023). This suggests that a non-laryngeal vocal source was present among the Dinosauria during at least the Late Jurassic, regardless of whether non-laryngeal vocalization is a plesiomorphy of Dinosauria or it is convergent in different dinosaur taxa (Yoshida et al. 2023). Even the fossilized syrinx could be found in the Mesozoic bird *Vegavis* (Clarke et al. 2016). Moreover, the possible complicated sound-making mechanism of *Pulaosaurus* suggests that individuals might have had relatively vocal or gregarious behavior.

Additionally, the preservation of ossified arytenoid in *Pulaosaurus* strongly suggests that ossification of the laryngeal apparatus has occurred not only in Ankylosauria and Aves (Yoshida et al. 2023) but also in Neornithischia. This indicates that ossified laryngeal apparatuses should have been phylogenetically widespread among non-avian dinosaurs. However, except for *Pulaosaurus* and *Pinacosaurus*, there are no other reports of ossified laryngeal apparatus preserved in non-avian dinosaur fossils. There are two probably explanations for this paucity of laryngeal anatomy within the non-avian dinosaur fossil record. Firstly, laryngeal elements are

gracile elements that rarely preserve or are taphonomically destroyed prior to discovery and description. Secondly, it is possible that other ossified laryngeal elements have been preserved, but have been misidentified (Yoshida et al. 2023). For example, the cricoids and arytenoids of *Pinacosaurus* were originally incorrectly identified as the paraglossals and the first pair of ceratobranchials (Hill et al. 2015). As described above, there have been many reports that there are two pairs of ceratobranchials in many dinosaur taxa which are defined as plate-like, splint-like, or ~~tetraiadiate~~ (Morschhauser 2013).. However, the second pair of ceratobranchials are lost in members of the extant archosaur phylogenetic bracket. It is highly possible that hyolaryngeal elements preserved in many non-avian dinosaur specimens that are currently identified as ceratobranchials are in fact ossified laryngeal elements. Reanalysis of vocal anatomy within non-avian dinosaurs needs to be carried out to assess the accuracy of identification among curated specimens.

Rod-like ceratobranchials are observed in *Pulaosaurus*. The length of *Pulaosaurus* ceratobranchials is less than 50% of the dentary length and their relative length is subequal to those of *Jeholosaurus* (Barrett 2009) but shorter than those of Paraves and quadrupedal ornithischians (Friedman et al. 2018). Elaborate ossified hyoid elements are typically observed in Aves, pterosaurs, and quadrupedal ornithischians such as ankylosaurids and hadrosauroids, which increases the mobility of the tongue and makes up for the diminished utility of forelimbs (Friedman et al. 2018). In pterosaurs, the ceratobranchials are elongated and fused. In Aves, epibranchials arise to increase the overall length of the hyoid element. In quadrupedal ornithischians, the frequency of ossification of hyoid elements increases (Friedman et al. 2018). The elongation of the ceratobranchials supports the mobility of the avian tongue (Friedman et al. 2018), which is closely associated with the feeding and ecological radiation of Aves. Similar

elaboration in hyoid elements is convergent in pterosaurs and certain quadrupedal ornithischians in which shifts of locomotion and diminished utility of forelimbs may introduce novel selective pressure to oral processing of food (Friedman et al. 2018).

The short relative length of *Pulaosaurus* ceratobranchials suggests that the tongue mobility of *Pulaosaurus* would have been limited. This may have been because *Pulaosaurus* ~~was~~ an obligate biped, ~~and its forelimbs could help with~~ food acquisition and processing. The limited tongue mobility and primitive tooth morphology of *Pulaosaurus* indicate that the food intraoral processing of *Pulaosaurus* is less prominent than later-diverging ornithischian taxa (Friedman et al. 2018) and it could only feed on softer food.

Conclusions

~~Conclusions~~

Pulaosaurus qinglong gen.et sp. nov. is the first Neornithischian species found in the Yanliao Biota placed at the base of ~~Neornothischia.~~ Preservation of its ossified laryngeal apparatus provides new information for the evolution of laryngeal apparatus in Archosaur, indicating that avian-like vocalization has appeared early and widely in non-avian dinosaurs.

Acknowledgements

Thanks first and foremost to Xing Xu for guidance and extensive access to the specimen. Yihui Ke and Rui Pei provide valuable advice for the previous drafts of this manuscript that has improved its quality greatly.

References

Bai C, Fan X, Li Z, Meng J, Zhu B. 2024. The first discovery of Middle Jurassic basalts in Northwestern Hebei Province and its geological significance. *Geological Review* 70(3):1127-1138.

Bailleul AM, O'Connor J, Li Z, Wu Q, Zhao T, Monleon MAM, Wang M, Zheng X. 2020.

1138 Confirmation of ovarian follicles in an enantiornithine (Aves) from the Jehol biota using
1139 soft tissue analyses. *Communications Biology* 3(1). 10.1038/s42003-020-01131-9
1140 Barrett PM, Butler RJ, Knoll F. 2005. Small-bodied ornithischian dinosaurs from the Middle
1141 Jurassic of Sichuan, China. *Journal of Vertebrate Paleontology* 25(4):823-834.
1142 10.1671/0272-4634(2005)025[0823:Sodftm]2.0.Co;2
1143 Barrett PM, Han F. 2009. Cranial anatomy of *Jeholosaurus shangyuanensis* (Dinosauria:
1144 Ornithischia) from the Early Cretaceous of China. *Zootaxa* 513(2072):31-55.
1145 10.5281/zenodo.187105
1146 Berta DE, Norell MA. 2021. The osteology of *Haya griva* (Dinosauria: Ornithischia) from the
1147 Late Cretaceous of Mongolia. *Bulletin of the American Museum of Natural History* 445(2021):1-
1148 111.
1149 Bonaparte JF, Novas FE, Coria RA. 1990. *Carnotaurus sastrei* Bonaparte, the horned, lightly
1150 built carnosaur from the Middle Cretaceous of Patagonia. *Contributions in science* 416:1-
1151 41. 10.5962/p.226819
1152 Boyd CA. 2014. The cranial anatomy of the neornithischian dinosaur *Thescelosaurus neglectus*.
1153 *PeerJ* 2(13): e669. 10.7717/peerj.669
1154 Boyd CA. 2015. The systematic relationships and biogeographic history of ornithischian
1155 dinosaurs. *PeerJ* 3(suppl): e1523. 10.7717/peerj.1523
1156 Brown CM, Boyd CA, Russell AP. 2011. A new basal ornithopod dinosaur (Frenchman
1157 Formation, Saskatchewan, Canada), and implications for late Maastrichtian ornithischian
1158 diversity in North America. *Zoological Journal of the Linnean Society* 163(4):1157-1198.
1159 10.1111/j.1096-3642.2011.00735.x
1160 Brown EE, Butler RJ, Barrett PM, Maidment SCR. 2022. Assessing conflict between early

1161 neornithischian tree topologies. *Journal of Systematic Palaeontology* 19(17):1183-1206.
1162 10.1080/14772019.2022.2032433
1163 Butler RJ. 2010. The anatomy of the basal ornithischian dinosaur *Eocursor parvus* from the
1164 lower Elliot Formation (Late Triassic) of South Africa. *Zoological Journal of the Linnean*
1165 *Society* 160(4):648-684. 10.1111/j.1096-3642.2009.00631.x
1166 Butler RJ, Jin L, Chen J, Godefroit P. 2011. The postcranial osteology and phylogenetic position
1167 of the small ornithischian dinosaur *Changchunsaurus parvus* from the Quantou
1168 Formation (Cretaceous: Aptian–Cenomanian) of Jilin Province, north-eastern China.
1169 *Palaeontology* 54(3):667-683. 10.1111/j.1475-4983.2011.01046.x
1170 Butler RJ, Upchurch P, Norman DB. 2008. The phylogeny of ornithischian dinosaurs. *Journal of*
1171 *Systematic Palaeontology* 6(1):1-40. 10.1017/S1477201907002271
1172 Clarke JA, Chatterjee S, Li Z, Riede T, Agnolin F, Goller F, Isasi MP, Martinioni DR, Mussel FJ,
1173 Novas FE. 2016. Fossil evidence of the avian vocal organ from the Mesozoic. *Nature*
1174 538(7626):502-505. 10.1038/nature19852
1175 Coria RA, Salgado L. 1996. A basal iguanodontian (Ornithischia: Ornithopoda) from the Late
1176 Cretaceous of South America. *Journal of Vertebrate Paleontology* 16(3):445-457.
1177 10.1080/02724634.1996.10011333
1178 Dieudonné PE, Cruzado-Caballero P, Godefroit P, Tortosa T. 2020. A new phylogeny of
1179 cerapodan dinosaurs. *Historical Biology* 33(10):2335-2355.
1180 10.1080/08912963.2020.1793979
1181 Forster C, Andrzejewski KA, Winkler DA, Jacobs LL. 2019. A new basal ornithopod
1182 (Dinosauria: Ornithischia) from the Early Cretaceous of Texas. *Plos One* 14(3):
1183 e0207935. 10.1371/journal.pone.0207935

1184 Friedman M, Li Z, Zhou Z, Clarke JA. 2018. Convergent evolution of a mobile bony tongue in
1185 flighted dinosaurs and pterosaurs. *Plos One* 13(6): e0198078.
1186 10.1371/journal.pone.0198078
1187 Galton PM. 1981. *Dryosaurus*, a hypsilophodontid dinosaur from the upper jurassic of north
1188 America and Africa postcranial skeleton. *Paläontologische Zeitschrift* 55(3-4):271-312.
1189 Galton PM, Upchurch P. 2004. Stegosauria. In: Weishampel DB, Dodson P, Osmólska H, eds.
1190 *The Dinosauria*. Second Edition. Berkeley: University of California Press, 343–362.
1191 Han F, Barrett PM, Bulter RJ, Xu X. 2012. Postcranial anatomy of *Jeholosaurus shangyuanensis*
1192 (Dinosauria: Ornithischia) from the Lower Cretaceous Yixian Formation of China.
1193 *Journal of Vertebrate Paleontology* 36(6):1370-1395.
1194 Han F, Foster CA, Xu X, Clark JM. 2017. Postcranial anatomy of *Yinlong downsi*(Dinosauria:
1195 Ceratopsia) from the Upper Jurassic Shishugou Formation of China and the phylogeny of
1196 basal ornithischians. *Journal of Systematic Palaeontology* 16(14):1159-1187.
1197 10.1080/14772019.2017.1369185
1198 He X, Cai K, Scientific S. 1984. The Middle Jurassic Dinosaurian Fauna from Dashanpu, Zigong,
1199 Sichuan Vol. I The Ornithopod Dinosaurs.
1200 Hill RV, D'Emic MD, Bever GS, Norell MA. 2015. A complex hyobranchial apparatus in a
1201 Cretaceous dinosaur and the antiquity of avian paraglossalia. *Zoological Journal of the*
1202 *Linnean Society* 175:892-909. 10.1111/zoj.12293
1203 Huang D. 2015. Yanliao Biota and Yanshan Movement. *Acta Palaeontologica Sinica* 54(4):501-
1204 546. 10.19800/j.cnki.aps.2015.04.008
1205 Huxley TH. 1870. On *Hypsilophodon Foxii*, a new Dinosaurian from the Wealden of the Isle of
1206 Wight. *Quarterly Journal of the Geological Society* 26(1-2):3-12.

1207 Jin L, Chen J, Zan S, Butler RJ, Godefroit P. 2010. Cranial anatomy of the small ornithischian
1208 dinosaur *Changchunsaurus parvus* from the Quantou Formation (Cretaceous: Aptian–
1209 Cenomanian) of Jilin Province, northeastern China. *Journal of Vertebrate Paleontology*
1210 30(1):196-214. 10.1080/02724630903412372
1211 Kingsley EP, Eliason CM, Riede T, Li Z, Hiscock TW, Farnsworth M, Thomson SL, Goller F,
1212 Tabin CJ, Clarke JA. 2018. Identity and novelty in the avian syrinx. *Proceedings of the*
1213 *National Academy of Sciences* 115(41):10209-10217. 10.1073/pnas.1804586115
1214 Kirchner JA. 1993. The vertebrate larynx: adaptations and aberrations. *The Laryngoscope*
1215 103:1197-1201.
1216 Krumenacker LJ. 2017. Osteology, phylogeny, taphonomy, and ontogenetic histology of
1217 *Oryctodromeus cubicularis*, from the middle Cretaceous (Albian-Cenomanian) of
1218 Montana and Idaho. Montana State University.
1219 Li N, Dai H, Tan C, Hu X, Wei Z, Lin Y, Wei G, Li D, Meng L, Hao B, You H, Peng G. 2019. A
1220 neornithischian dinosaur from the Middle Jurassic Xintiangou Formation of Yunyang,
1221 Chongqing, China: the earliest record in Asia. *Historical Biology* 33(7):1089-1102.
1222 10.1080/08912963.2019.1679129
1223 Liu F, Wu R, Han F. 2022. Vertebrate diversity of the Yanliao Biota and comparison with other
1224 biotas *Acta Palaeontologica Sinica* 61(1):88-106. 10.19800/j.cnki.aps.2020027
1225 Madzia D, Arbour VM, Boyd CA, Farke AA, Cruzado-Caballero P, Evans DC. 2021. The
1226 phylogenetic nomenclature of ornithischian dinosaurs.*PeerJ*9:e12362. DOI
1227 10.7717/peerj.12362
1228 Min H, Lee DG, Kim JK, Lim JD, Godefroit P. 2011. A new basal ornithopod dinosaur from the
1229 Upper Cretaceous of South Korea. *Neues Jahrbuch für Geologie und Paläontologie* -

1230 *Abhandlungen* 259(1):1-24. 10.1127/0077-7749/2010/0102
1231 Molnar RE, Clifford HT. 2000. Gut contents of a small ankylosaur. *Journal of Vertebrate*
1232 *Paleontology* 20(1):194-196. 10.1671/0272-4634(2000)020[0194:Gcoasa]2.0.Co;2
1233 Morschhauser EM, Lamana MC. 2013. A Reevaluation of the Hyoid Bones of *Protoceratops*
1234 *andrewsi* Granger and Gregory, 1923 (Ornithischia: Ceratopsia) and a Review of Hyoid
1235 Elements in Ornithischian Dinosaurs. *Annals of Carnegie Museum* 81(4):247-255.
1236 10.2992/007.081.0404
1237 Norman DB, Crompton AW, Butler RJ, Porro LB, Charig AJ. 2011. The Lower Jurassic
1238 ornithischian dinosaur *Heterodontosaurus tucki* Crompton & Charig, 1962: cranial
1239 anatomy, functional morphology, taxonomy, and relationships. *Zoological Journal of the*
1240 *Linnean Society* 163(1):182-276. 10.1111/j.1096-3642.2011.00697.x
1241 Norman DB, Sues HD, Witmer LM, Coria RA. 2004. Basal Ornithopoda. In: Weishampel DB,
1242 Dodson P, Osmólska H, eds. *The Dinosauria*. Second Edition. Berkeley: University of
1243 California Press, 393–412.
1244 O'Connor JK, Zheng X, Wang X, Wang Y, Zhou Z. 2014. Ovarian follicles shed new light on
1245 dinosaur reproduction during the transition towards birds. *National Science Review*
1246 1(1):15-17. 10.1093/nsr/nwt012
1247 Peng G. 1992. Jurassic Onrithopod *Agilisaurus louderbacki*(Ornithopoda: Fabrosauridae) from
1248 Zigong, Sichuan, China. *Vertebrae Palasiatica* 30(1):39-53.
1249 Prieto-Márquez A, and Norell MA. 2010. Anatomy and Relationships of *Gilmoreosaurus*
1250 *mongoliensis*(Dinosauria: Hadrosauroidea) from the Late Cretaceous of Central Asia.
1251 *American Museum Novitates* 3694:1-49. 10.1206/3694.2
1252 Riede T, Li Z, Tokuda IT, Farmer CG. 2015. Functional morphology of the *Alligator*

mississippiensis larynx with implications for vocal production. *Journal of Experimental Biology* 218(7):991-998. 10.1242/jeb.117101

Ruiz-Omeñaca JI, Canudo JI, Cuenca-Bescós G, Cruzado-Caballero P, Gasca JM, Moreno-Azanza M. 2012. A new basal ornithopod dinosaur from the Barremian of Galve, Spain. *Comptes Rendus Palevol* 11(6):435-444. 10.1016/j.crpv.2012.06.001

Sacchi R, Galeotti P, Fasola M, Gerzeli G. 2004. Larynx morphology and sound production in three species of Testudinidae. *Journal of Morphology* 261(2):175-183. 10.1002/jmor.10236

Scheetz RD. 1999. Osteology of *Orodromeus makelai* and the phylogeny of basal ornithopod dinosaurs. Montana State University.

Sereno P. 1991. *Lesothosaurus*, "Fabrosaurids," and the early evolution of Ornithischia. *Journal of Vertebrate Paleontology* 11(2):168-197. 10.1080/02724634.1991.10011386

Sober S, Riede T, Thomson SL, Titze IR, Goller F. 2019. The evolution of the syrinx: An acoustic theory. *PLOS Biology* 17(2): e2006507. 10.1371/journal.pbio.2006507

Wang Y, Wang M, O'Connor JK, Wang X, Zheng X, Zhang X. 2016. A new Jehol enantiornithine bird with three-dimensional preservation and ovarian follicles. *Journal of Vertebrate Paleontology* 36(2): e1054496. 10.1080/02724634.2015.1054496

Winkler DA, Murry PA, Jacobs LL. 1997. A new species of *Tenontosaurus* (Dinosauria: Ornithopoda) from the Early Cretaceous of Texas. *Journal of Vertebrate Paleontology* 17(2):330-348.

Xu X, Clark JM, Eberth DA, Currie PJ. 2022. The Shishugou Fauna of the Middle-Late Jurassic Transition Period in the Junggar Basin of Western China. *Acta Geologica Sinica - English Edition* 96(4):1115-1135. 10.1111/1755-6724.14996

1276 Yang Y, Wu W, Dieudonné PE, Godefroit P. 2020. A new basal ornithopod dinosaur from the
1277 Lower Cretaceous of China. *PeerJ* 8: e9832. 10.7717/peerj.9832
1278 Yoshida J, Kobayashi Y, Norell MA. 2023. An ankylosaur larynx provides insights for bird-like
1279 vocalization in non-avian dinosaurs. *Communications Biology* 6(1). 10.1038/s42003-023-
1280 04513-x
1281 You H, Dodson P. 2004. Basal Ceratopsia. In: Weishampel DB, Dodson P, Osmólska H, eds.
1282 *The Dinosauria*. Second Edition. Berkeley: University of California Press, 478–493.
1283 Zhou ZH, Wang Y. 2017. Vertebrate assemblages of the Jurassic Yanliao Biota and the Early
1284 Cretaceous Jehol Biota: Comparisons and implications. *Palaeoworld* 26(2):241-252.
1285 10.1016/j.palwor.2017.01.002
1286

Figure 1

Photograph of the whole skeleton of *Pulaosaurus qinglong* in left lateral view (IVPP V30936)

Figure 2

The skull of *Pulaosaurus qinglong* in left lateral view (IVPP V30936).

(A) Photograph. (B) Outline drawing

Abbreviations:

ang-angular; art-articular; ary-arytenoid; at int-atlas intercentrum; bo-basioccipital; bsp-basisphenoid; cera-ceratobranchial; cr-cervical rib; ecp-ectopterygoid; exo-exoccipital; fr-frontal; j-jugal; jb-jugal boss; lcr-lacrimal; ld-left dentary; lsp?-laterosphenoid?; l spl-left splenial; m-maxilla; ms-Meckelian sulcus; na-nasal; nc-nuchal crest; nf-nutrient foramina; od p-odontoid process; p-pterygoid; pa-parietal; pal-palatine; par-parapophysis; par p-paraoccipital process; pb-palpebral; po-postorbital; pp-pterygoid process of basisphenoid; prd-predentary; prf-prefrontal; prm-premaxilla; sq-squamosal; q-quadrate; qj-quadratojugal; rd-right dentary; r spl-right splenial; spo-supraoccipital; sur-surangular.

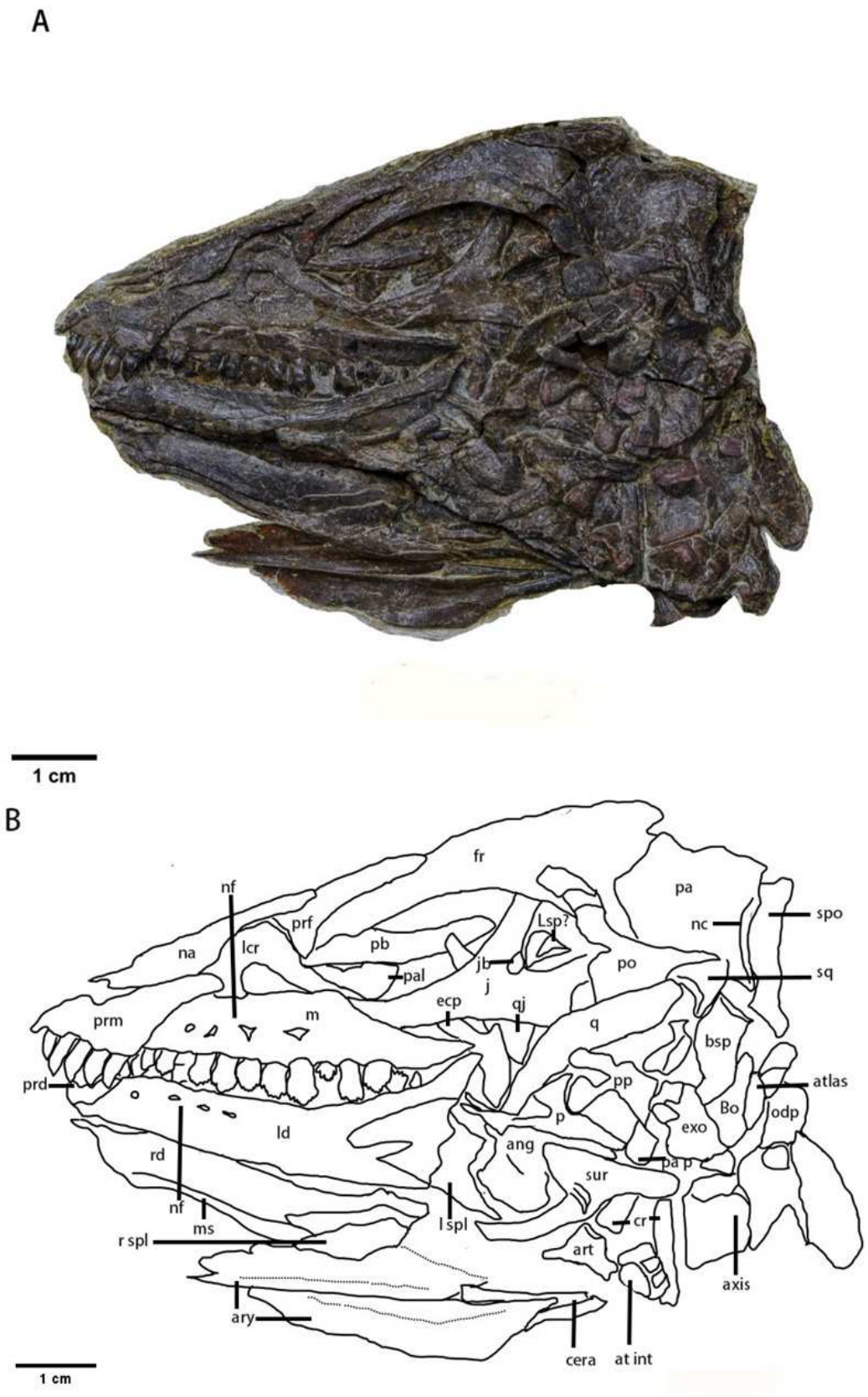
A
1 cm
B
fr
nf
pa
prf
Lsp?
nc
spo
na
lcr
pb
jb
po
sq
pal
j
ecp
qj
prm
m
q
bsp
prd
pp
atlas
Bo
odp
p
exo
ld
ang
rd
pa p
sur
nf
ms
l spl
cr
r spl
art
axis
ary
cera
at int
1 cm

Figure 3

Arytenoids and ceratobranchials of *Pulaosaurus qinglong* in laterodorsal view (IVPP V30936)

(A) The photograph of ceratobranchials and arytenoids. (B) The line drawing of ceratobranchials and arytenoids.

Abbreviations:

ap-arytenoid process; c-ceratobranchial; lw-laterodorsal wings of the arytenoids; mw-mediodorsal wings of the arytenoids.

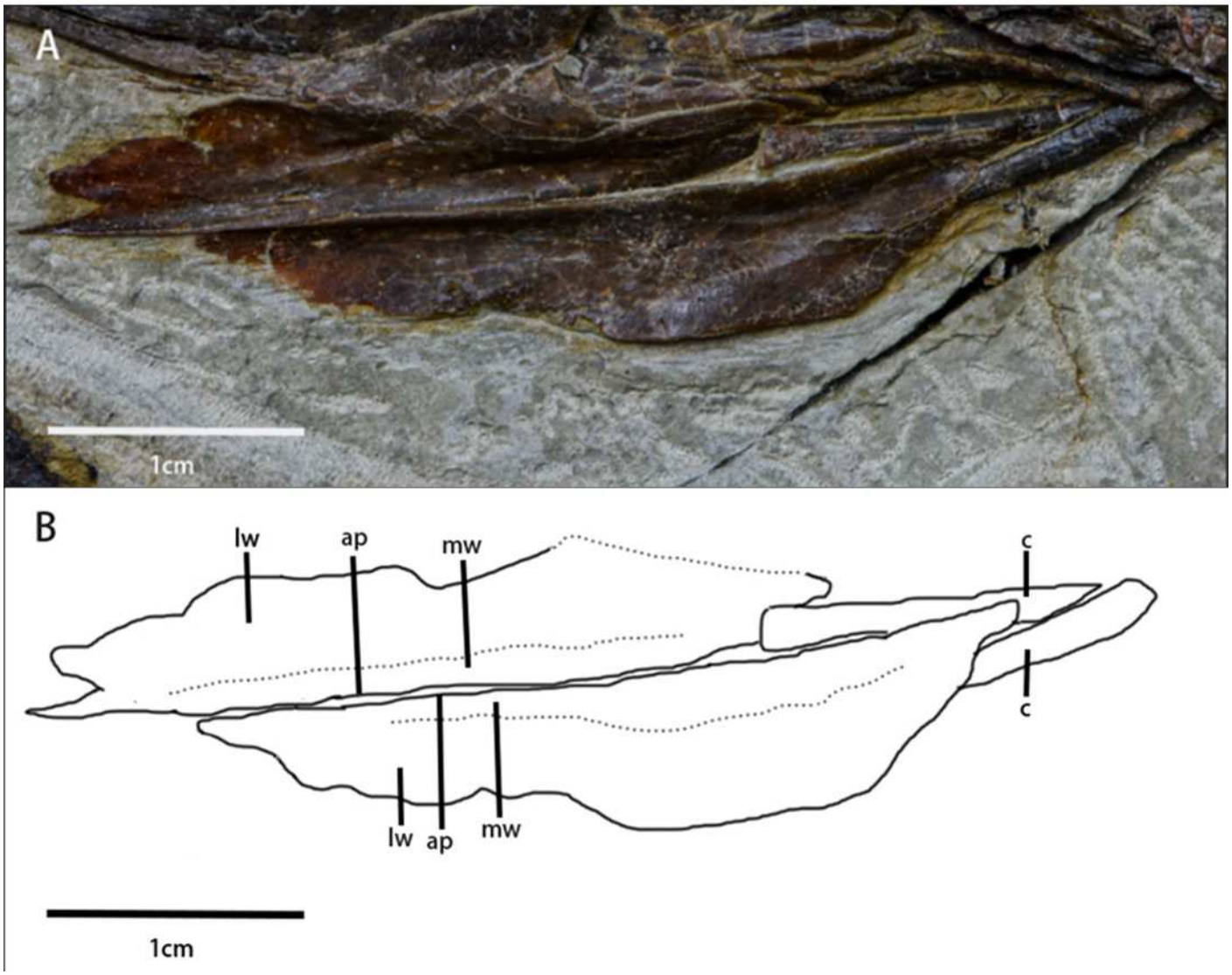
A
1cm
B
lw
ap
mw
c
c
lw
ap
mw
1cm

Figure 4

Cervical Series of *Pulaosaurus qinglong*: (IVPP V30936). Atlas, axis and 3rd cervical visible in left lateral view; from 4th cervical to 9th cervical visible in dorsal view.

(A) The photograph of the cervical series. (B) The line drawing of the cervical series.

Abbreviation:

a int-axis intercentrum; cr-cervical rib; dia-diapophysis; ns-neural spine; od p-odontoid process; pa-parapophysis; pop-postzygapophysis; tp-transverse process.

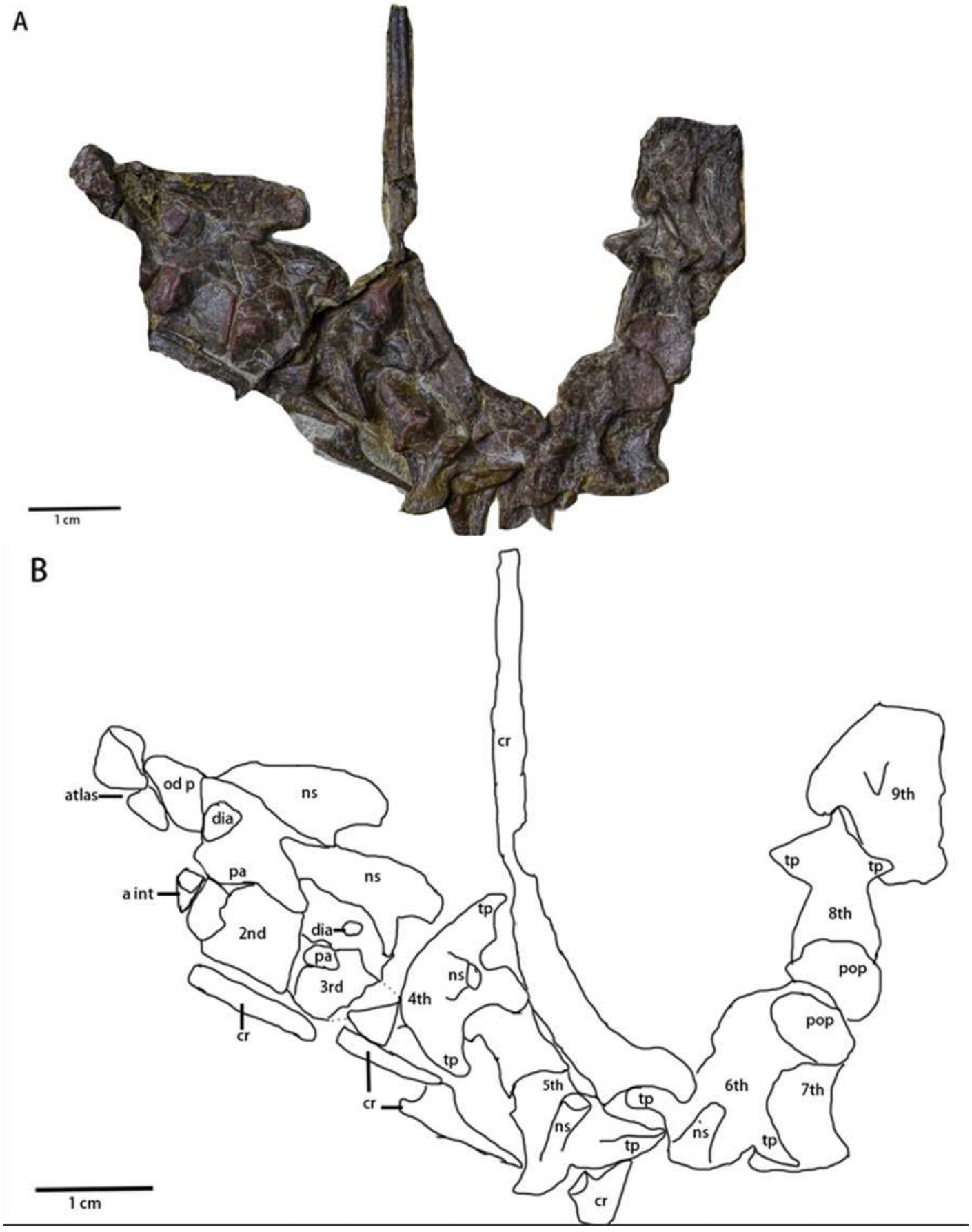
A
1 cm
B
atlas
od p
ns
dia
pa
ns
a int
2nd
dia
pa
3rd
cr
cr
cr
tp
ns
4th
tp
5th
ns
tp
cr
6th
tp
ns
7th
tp
pop
pop
8th
tp
tp
9th
1 cm

Figure 5

Dorsal vertebrae and ossified tendons of *Pulaosaurus qinglong* in left lateral view (IVPP V30936).

(A) The photograph of ossified tendons. (B) The photograph of posterior dorsal vertebrae. (C) The photograph of ribs articulating with dorsal vertebrae.

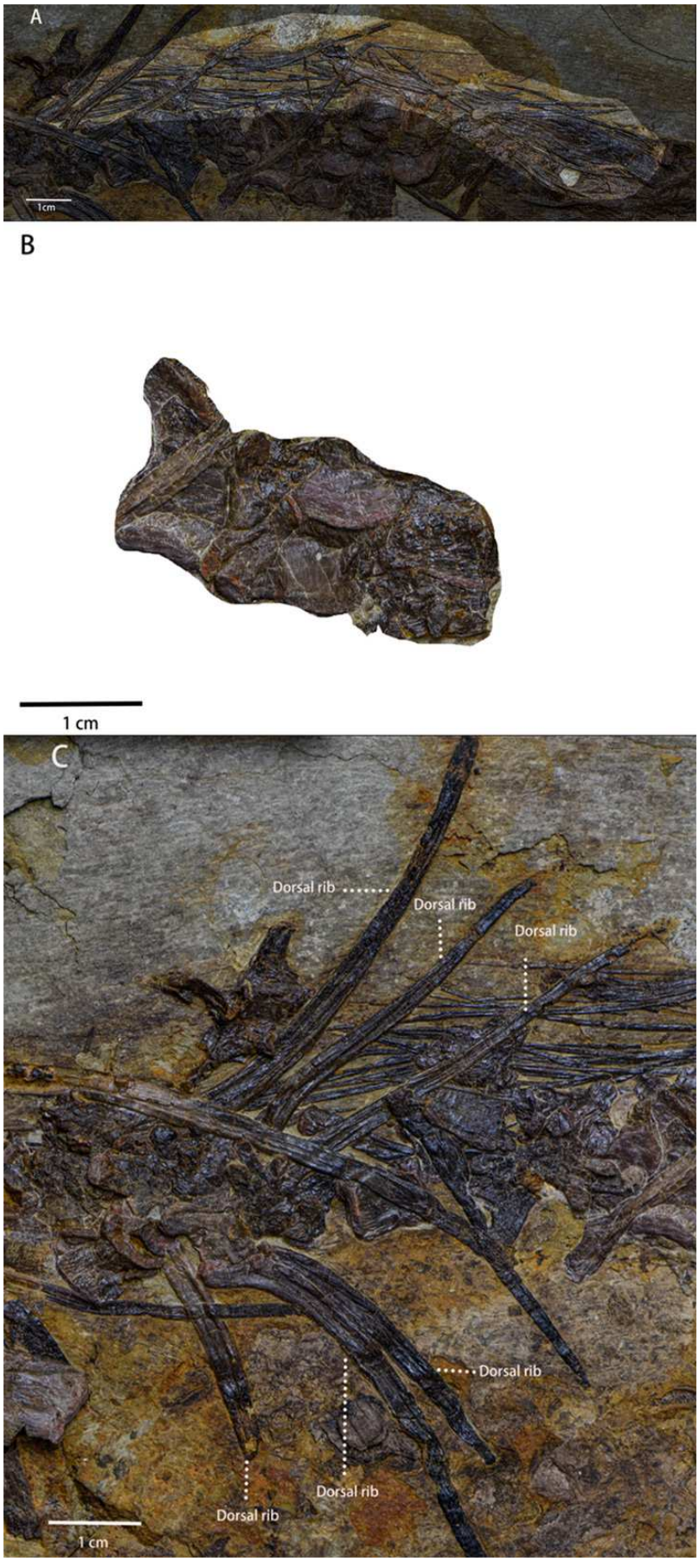
A
1cm
B
1 cm
C
Dorsal rib
Dorsal rib
Dorsal rib
Dorsal rib
Dorsal rib
Dorsal rib
1 cm

Figure 6

Caudal vertebrae series of *Pulaosaurus qinglong* in left lateral view (IVPP V30936).

(A) Anterior caudal vertebrae. (B) Middle caudal vertebrae. (C) Posterior caudal vertebrae.

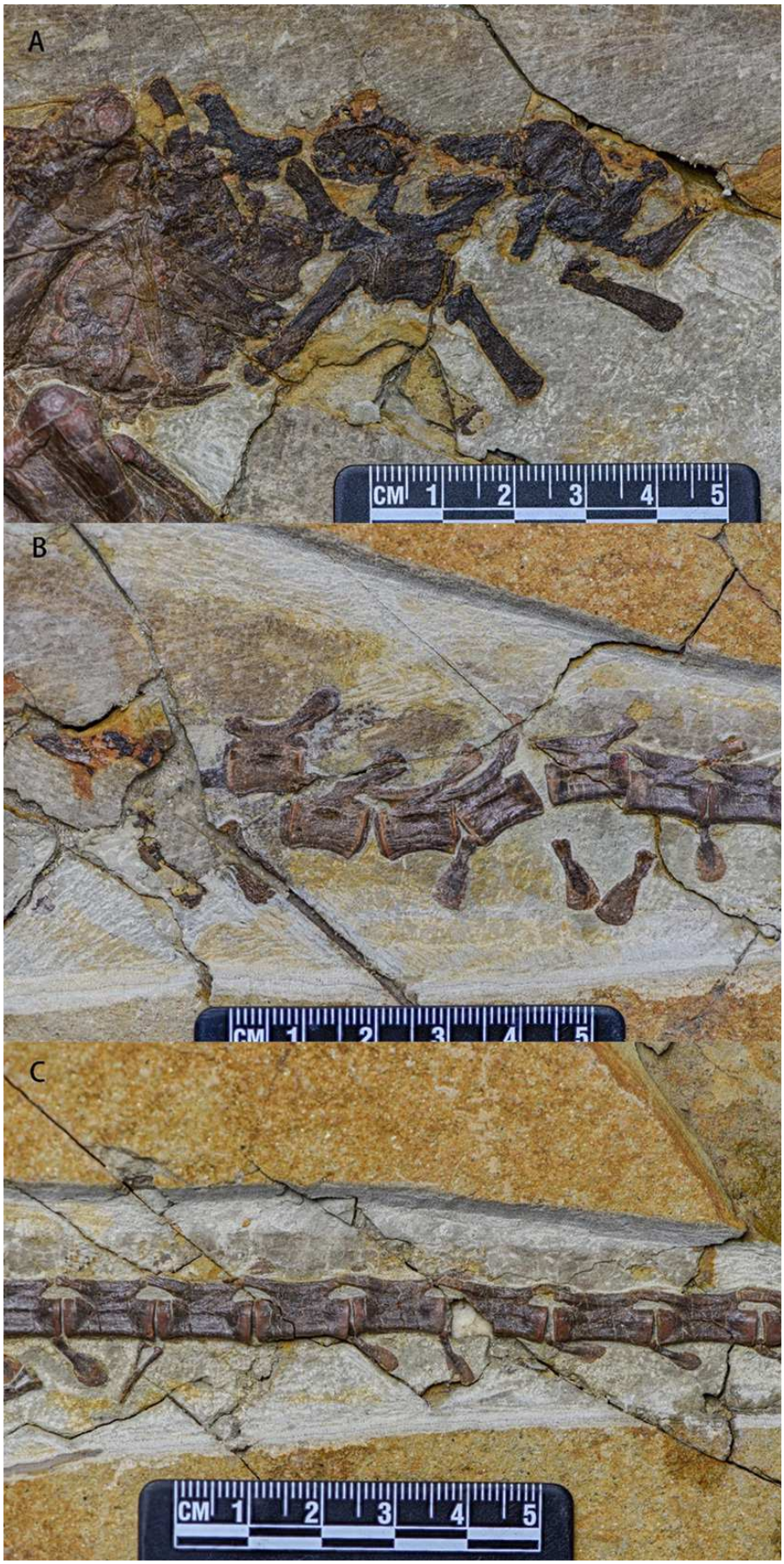
A
CM 1 2 3 4 5
B
CM 1 2 3 4 5
C
CM 1 2 3 4 5

Figure 7

Pectoral girdle and sternum of *Pulaosaurus qinglong* (IVPP V30936) in left lateral view.

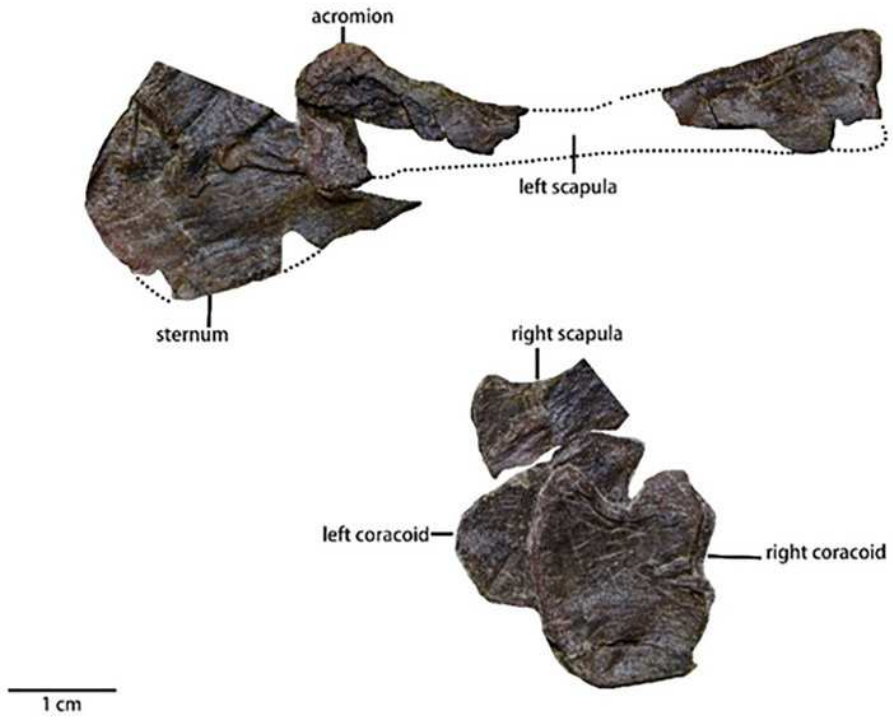

Figure 8

Left forelimb of *Pulaosaurus qinglong* in left lateral view (IVPP V30936).

(A) L eft humerus. (B) L eft ulna, radius, and manus.

Abbreviations:

dc-distal carpal; int-intermedium.

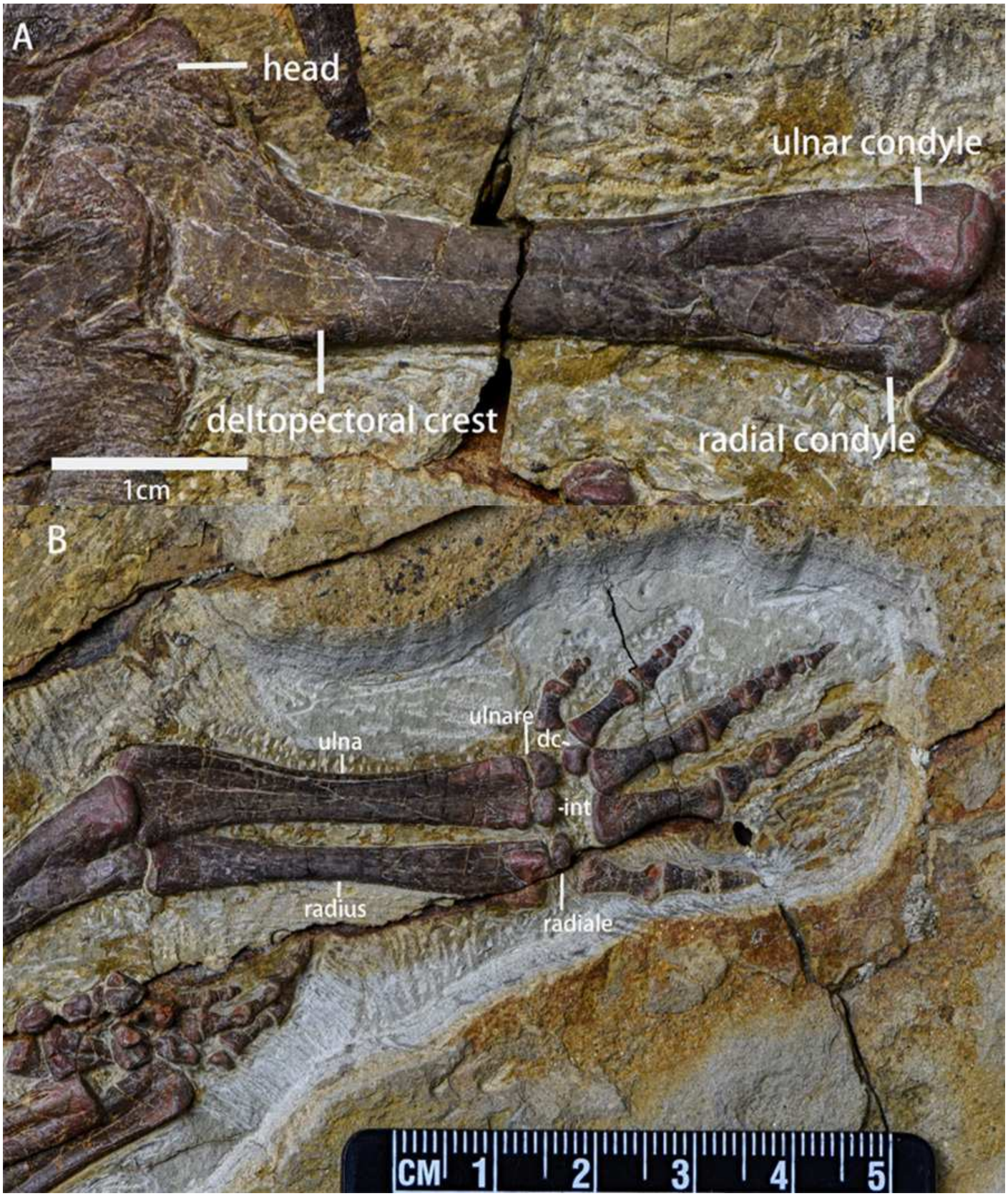
A
head
ulnar condyle
deltopectoral crest
radial condyle
1cm
B
ulnare
dc
ulna
int
radius
radiale
CM 1 2 3 4 5

Figure 9

The pelvic girdle of *Pulaosaurus qinglong* in left lateral view (IVPP V30936).

(A) The photograph of the left ilium. (B) The line drawing of the left ilium. (C) The photograph of the pubis and the ischium, scale bar: 1cm. (D) The CT image of the pubis and the ischium.

Abbreviation:

bf-brevis fossa; ip-ischiac peduncle; isc-ischium; of-obturator foramen; opi-obturator process of the ischium; pop-postacetabular process; prep-preacetabular process; pup-pubic peduncle; sc-supra-acetabular crest.

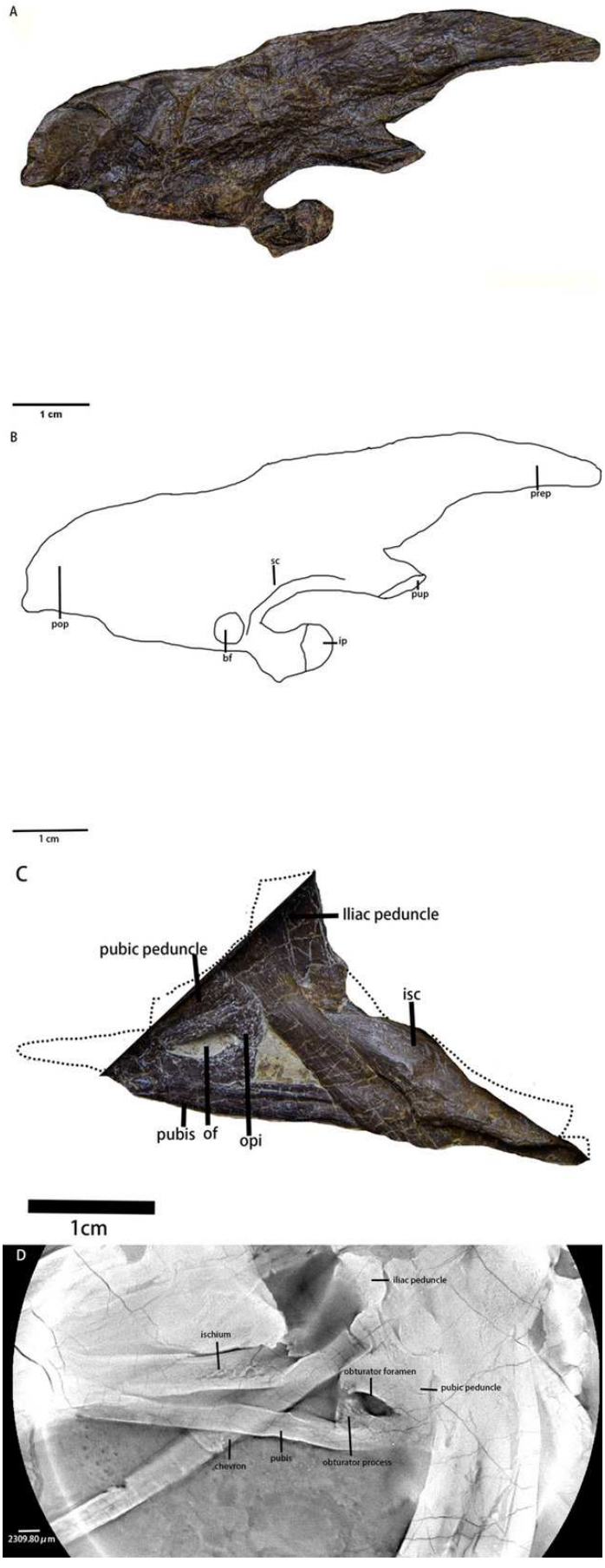
A
1 cm
B
prep
sc
pup
pop
bf
ip
1 cm
C
Iliac peduncle
pubic peduncle
isc
pubis
of
opi
1cm
D
iliac peduncle
ischium
obturator foramen
pubic peduncle
chevron
pubis
obturator process
2309.80 µm

Figure 10

The femora of *Pulaosaurus qinglong* (IVPP V30936).

(A) The left femur in medial view. (B) The right femur in medial view.

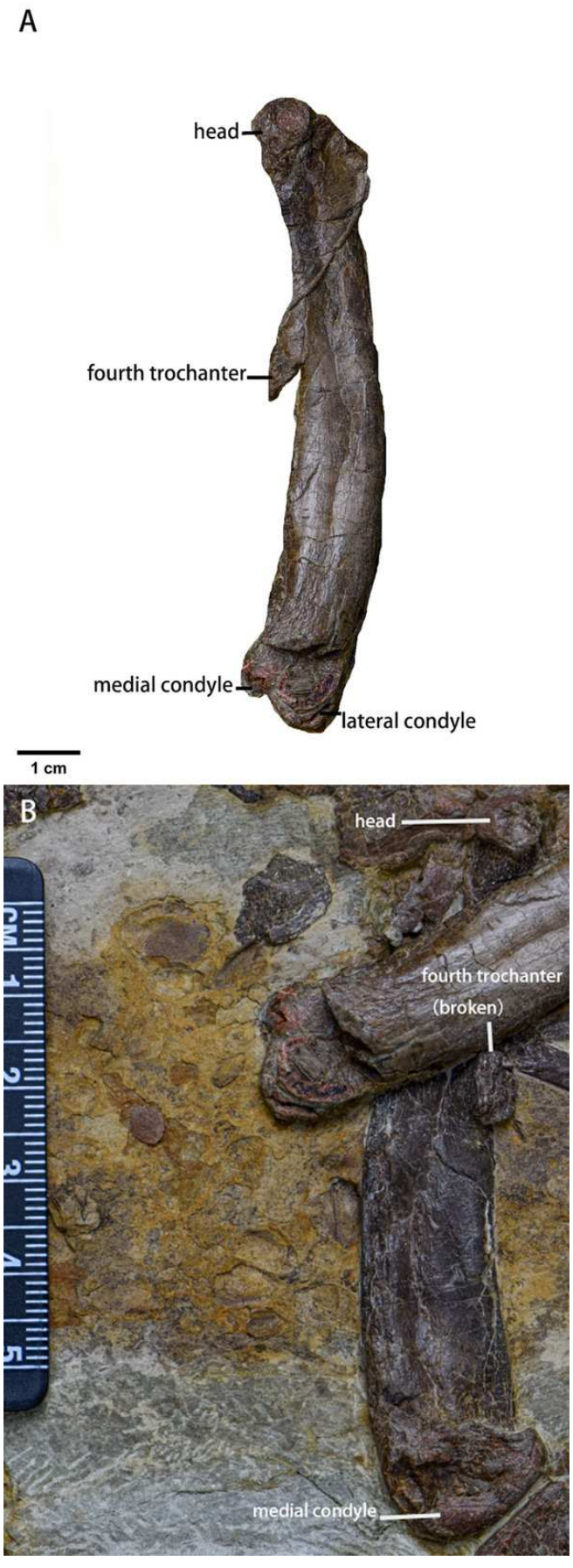
A
head
fourth trochanter
medial condyle
lateral condyle
1 cm
B
head
fourth trochanter
(broken)
medial condyle

Figure 11

Left tibia and fibula of *Pulaosaurus qinglong* in anterior view (IVPP V30936).


inner condyle
fibula condyle
cnemial crest
Incisura tibialis
-fibula
tibia
internal malleolus
external malleolus
CM 1 2 3 4 5

Figure 12

Astragali, calcaneum and pedes of *Pulaosaurus qinglong* (IVPP V30936).

(A) Right astragalus, calcaneum, metatarsals in dorsal view and phalanges in lateroventral view. (B) Left astragalus in dorsal view, metatarsals in ventral view and phalanges in lateral view.

Abbreviations: ast-astragalus, cal-calcaneum, dt-distal tarsal, mt-metatarsal, I-1-phalanx I-1, I-2-phalanx I-2, II-1-phalanx II-1, II-2-phalanx II-2, II-3-phalanx II-3, III-1-phalanx III-1, III-2-phalanx III-2, III-3-phalanx III-3, III-4-phalanx III-4, IV-1-phalanx IV-1, IV-2-phalanx IV-2, IV-3-phalanx IV-3, IV-4-phalanx IV-4, IV-5-phalanx IV-5.

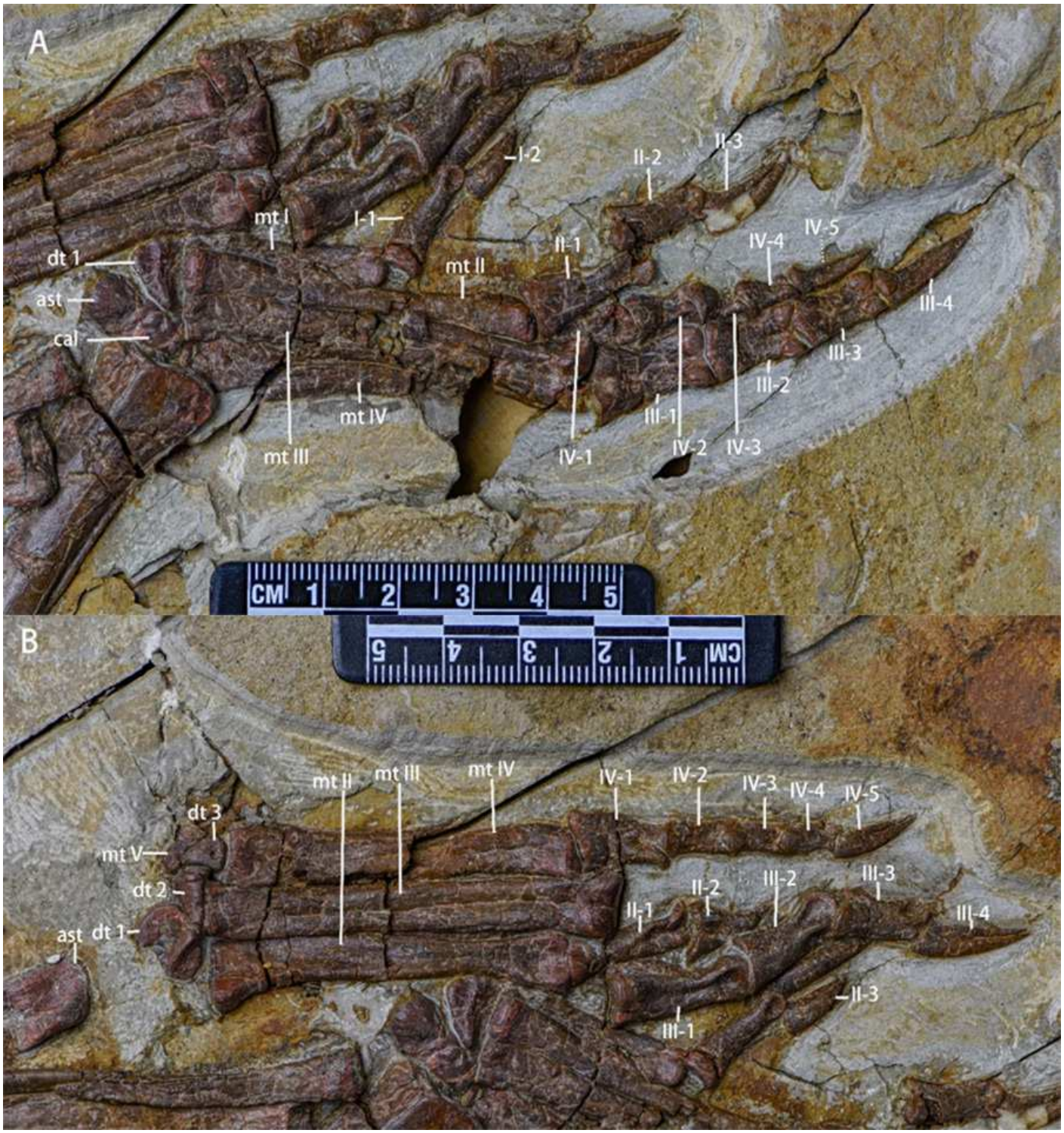
A
I-2
II-2
II-3
mt I
I-1
dt 1
ast
cal
II-1
mt II
IV-4
IV-5
III-4
III-3
III-2
mt IV
III-1
mt III
IV-1
IV-2
IV-3
CM 1 2 3 4 5
B
mt II
mt III
mt IV
IV-1
IV-2
IV-3
IV-4
IV-5
dt 3
mt V
dt 2
III-2
III-3
II-2
II-1
III-4
ast
dt 1
II-3
III-1

Figure 13

Cololites of *Pulaosaurus qinglong* (IVPP V30936).


CM
1
2
3
4
5

Figure 14

The strict consensus tree from 19,701 most parsimonious trees including 74 taxa and 380 characters generated by the analysis.

Nodes: 1-Ornithischia, 2-Pachycephalosauria, 3-Iguanodontia, 4-Neoceratopsia , 5-Thyreophora.

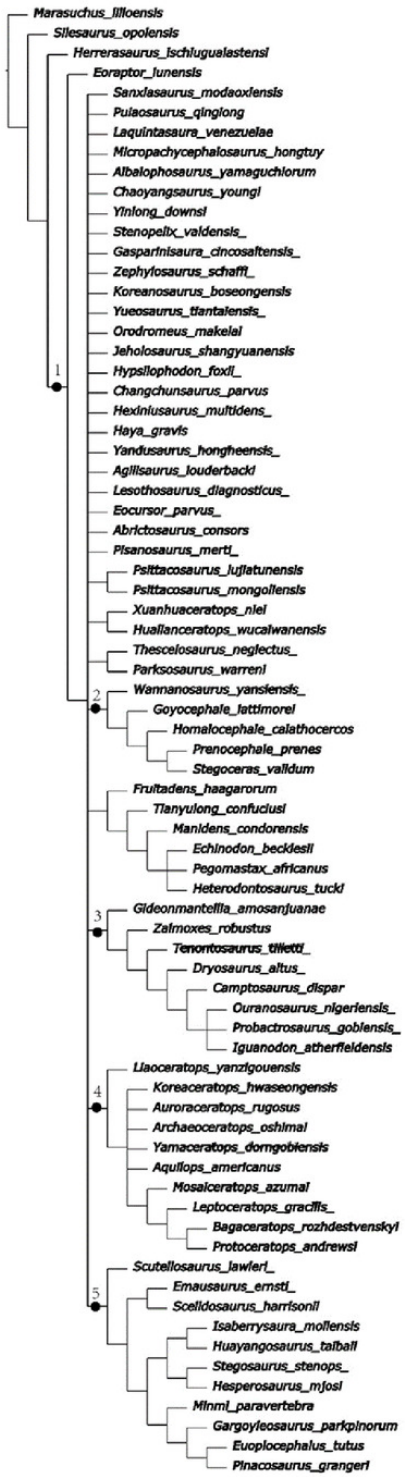
Marasuchus_lilloensis
Sllesaurus_opolensis
Herrerasaurus_ischigualastensi
Eoraptor_lunensis
Sanxiasaurus_modaoxiensis
Pulaosaurus_qinglong
Laquintasaura_venezuelae
Micropachycephalosaurus_hongtuy
Albalophosaurus_yamaguchiorum
Chaoyangsaurus_youngi
Yinlong_downsi
Stenopelix_valdensis_
Gasparinisaura_cincosaltensis_
Zephyrosaurus_schaffi_
Koreanosaurus_boseongensis
Yueosaurus_tiantaiensis_
Orodromeus_makelai
Jeholosaurus_shangyuanensis
Hypsilophodon_foxi_
Changchunsaurus_parvus
Hexinlusaurus_multidens_
Haya_gravis
Yandusaurus_hongheensis_
Agilisaurus_louderbacki
Lesothosaurus_diagnosticus_
Eocursor_parvus_
Abrictosaurus_consors
Pisanosaurus_merti_
Psittacosaurus_lujiatunensis
Psittacosaurus_mongoliensis
Xuanhuaceratops_niei
Huallanceratops_wucaiwanensis
Thescelosaurus_neglectus_
Parksosaurus_warreni
Wannanosaurus_yansiensis_
Goyocephale_lattimorei
Homalocephale_calathocercos
Prenocephale_prenes
Stegoceras_validum
Fruitadens_haagarorum
Tianyulong_confuciusi
Manidens_condorensis
Echinodon_becklesii
Pegomastax_africanus
Heterodontosaurus_tucki
Gideonmantellia_amosanjuanae
Zalmoxes_robustus
Tenontosaurus_tilletti_
Dryosaurus_altus_
Camptosaurus_dispar
Ouranosaurus_nigeriensis_
Probactrosaurus_gobiensis_
Iguanodon_atherfieldensis
Liaoceratops_yanzigouensis
Koreaceratops_hwaseongensis
Auroraceratops_rugosus
Archaeoceratops_oshimai
Yamaceratops_dorngobiensis
Aquilops_americanus
Mosaiceratops_azumai
Leptoceratops_gracilis_
Bagaceratops_rozhdestvenskyi
Protoceratops_andrewsi
Scutellosaurus_lawleri_
Emausaurus_ernsti_
Scelidosaurus_harrisonii
Isaberrysaura_mollensis
Huayangosaurus_taibaii
Stegosaurus_stenops_
Hesperosaurus_mjosi
Minmi_paravertebra
Gargoyleosaurus_parkpinorum
Euoplocephalus_tutus
Pinacosaurus_grangeri
1
2
3
4
5

Figure 15

The reduced strict consensus tree from 500 most parsimonious trees including 67 taxa and 380 characters generated by the analysis.

Nodes □

1-Ornithischia, 2-Heterodontosauridae, 3-Genasauria, 4-Thyreophora, 5-Neornithischia, 6-Cerapoda, 7-Ornithopoda, 8-Iguanodontia, 9-Marginocephalia, 10-Pachycephalosauria, 11-Ceratopsia, 12-Chaoyangsauridae, 13-Neoceratopsia.

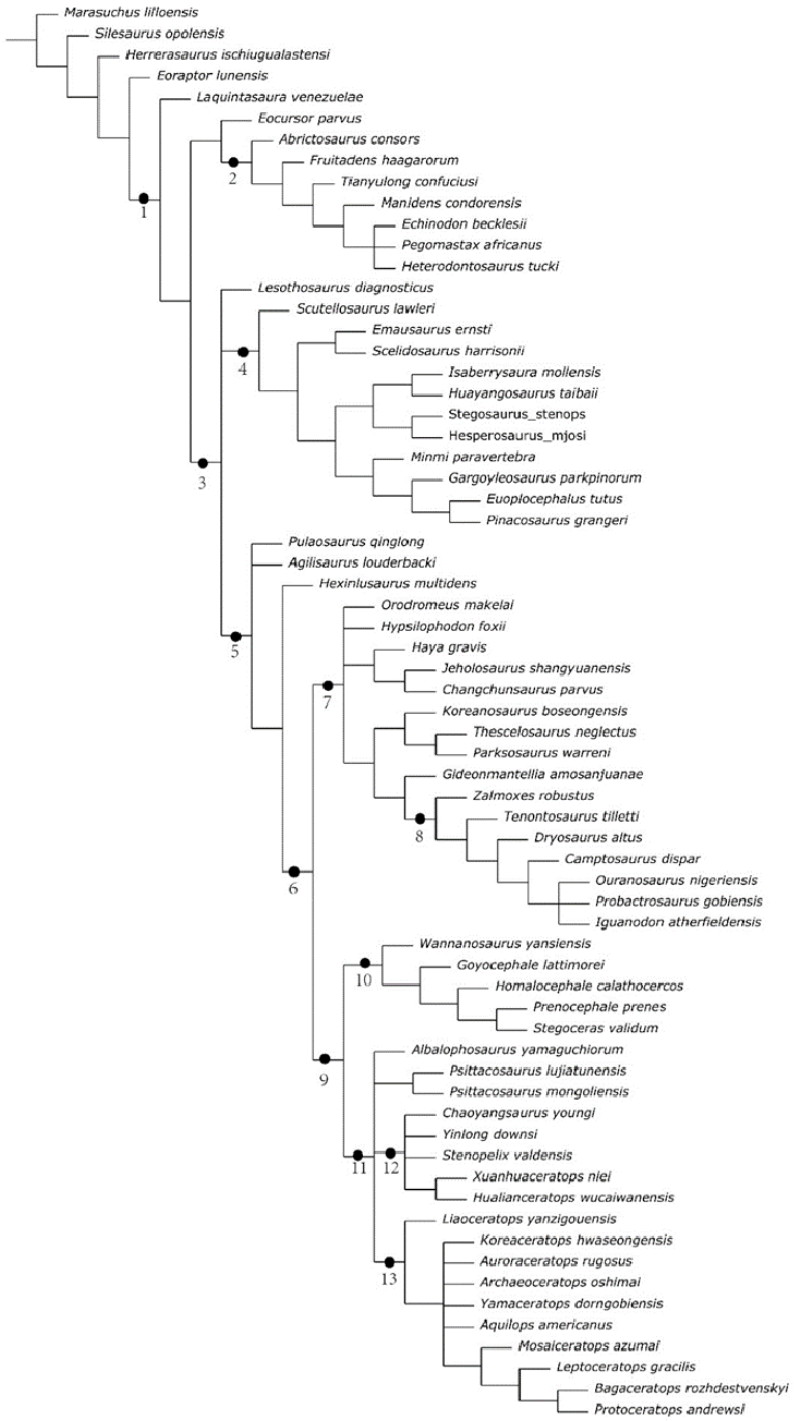
Marasuchus lilloensis
Silesaurus opolensis
Herrerasaurus ischigualastensi
Eoraptor lunensis
Laquintasaura venezuelae
Eocursor parvus
Abrictosaurus consors
Fruitadens haagarorum
Tianyulong confuciusi
Manidens condorensis
Echinodon becklesii
Pegomastax africanus
Heterodontosaurus tucki
Lesothosaurus diagnosticus
Scutellosaurus lawleri
Emausaurus ernsti
Scelidosaurus harrisonii
Isaberrysaura mollensis
Huayangosaurus taibaii
Stegosaurus_stenops
Hesperosaurus_mjosi
Minmi paravertebra
Gargoyleosaurus parkpinorum
Euoplocephalus tutus
Pinacosaurus grangeri
Pulaosaurus qinglong
Agilisaurus louderbacki
Hexinlusaurus multidens
Orodromeus makelai
Hypsilophodon foxii
Haya gravis
Jeholosaurus shangyuanensis
Changchunsaurus parvus
Koreanosaurus boseongensis
Thescelosaurus neglectus
Parksosaurus warreni
Gideonmantellia amosanjuanae
Zalmoxes robustus
Tenontosaurus tilletti
Dryosaurus altus
Camptosaurus dispar
Ouranosaurus nigeriensis
Probactrosaurus gobiensis
Iguanodon atherfieldensis
Wannanosaurus yansiensis
Goyocephale lattimorei
Homalocephale calathocercos
Prenocephale prenes
Stegoceras validum
Albalophosaurus yamaguchiorum
Psittacosaurus lujiatunensis
Psittacosaurus mongoliensis
Chaoyangsaurus youngi
Yinlong downsi
Stenopelix valdensis
Xuanhuaceratops niei
Hualianceratops wucaiwanensis
Liaoceratops yanzigouensis
Koreaceratops hwaseongensis
Auroraceratops rugosus
Archaeoceratops oshimai
Yamaceratops dorngobiensis
Aquilops americanus
Mosaiceratops azumai
Leptoceratops gracilis
Bagaceratops rozhdestvenskyi
Protoceratops andrewsi
1
2
3
4
5
6
7
8
9
10
11
12
13

Figure 16

Evolution of hyolaryngeal elements in Archosauria. The figure is adapted from illustration by Tatsuya Shinmura [24] .

The figure is adapted from illustration by Tatsuya Shinmura [24] .

Yellow-arytenoid, green-first pair of ceratobranchials, black-second pair of ceratobranchials, red-cricoid, white-basihyal, blue-procricoid, orange-paraglossal, grey-epibranchials.

Numbers represent the ancestral state of characteristics: 1-Laryngeal vocal source, 2-Loss of second ceratobranchials, 3-Procrocoid, 4-Arytenoid process, 5- Arytenoid process, 6-Ossified larynx, 7-Immobile lungs, 8-Procrocoid, 9-Paraglossal.

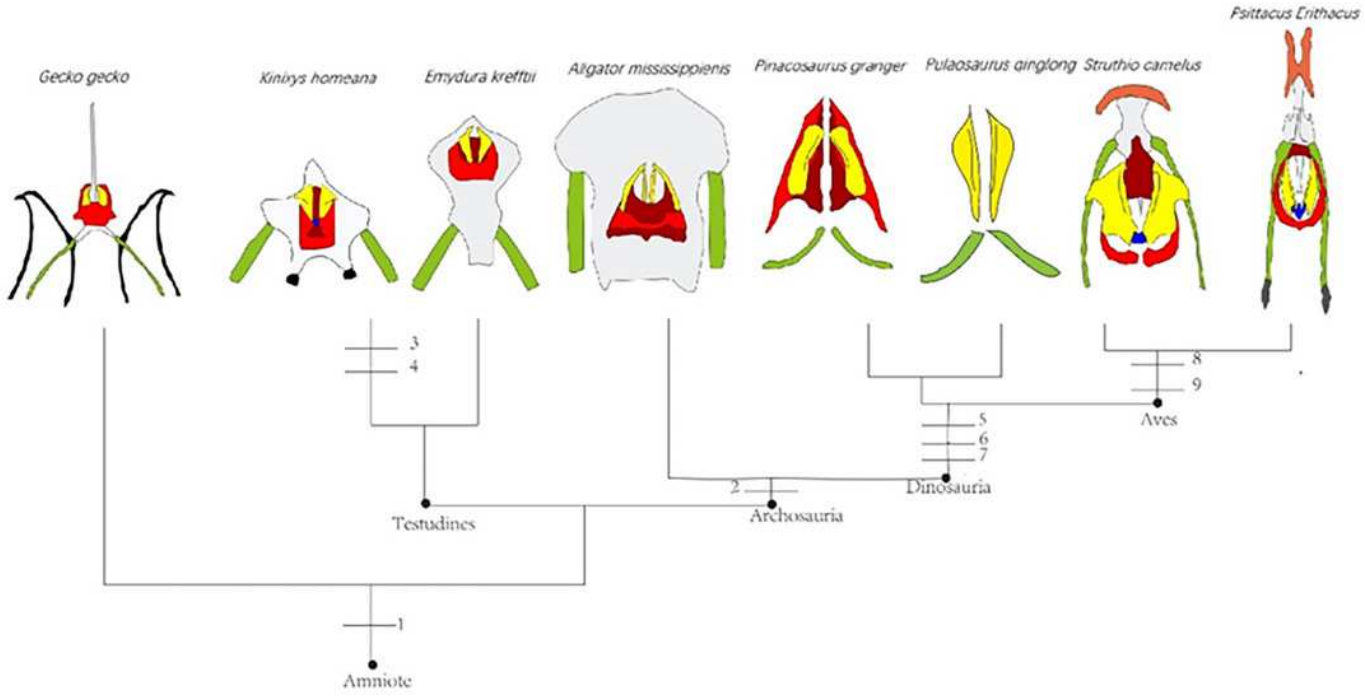

Table 1(on next page)

Measurements of *Pulaosaurus qinglong* specimen V30936 skull elements.

1

Skull length	82mm
Skull height	42mm
Orbit maximal diameter	30.14mm
Preorbital skull length	30.84mm
Supratemporal fenestra length	15.24mm
Frontal length	36.92mm
Frontal minimal width	14.60mm
Dentary length	39.48mm
Right arytenoid length	31.9mm
Right arytenoid maximal width	5.8mm
Left arytenoid length	34.3mm
Left arytenoid maximal width	6.2mm
Right ceratobranchial length（visible part）	13.8mm
Left ceratobranchial length（visible part）	10.0mm

2 Table 1 Measurements of *Pulaosaurus qinglong* specimen V30936 skull elements

3

Table 2(on next page)

Measurements of *Pulaosaurus qinglong* specimen V30936 cervical series.

Axial length	8.50mm
3rd cervical centrum length	9.04mm
4th cervical centrum length	12.76mm
5th cervical centrum length	?
6th cervical centrum length	15.62mm
7th cervical centrum length	?
8th cervical centrum length	?
9th cervical centrum length	?

1

Table 3(on next page)

Measurements of *Pulaosaurus qinglong* specimen V30936 coracoids.

Right coracoid length in medial view	19.86mm
Right coracoid maximal width in medial view	16.68mm
Left coracoid length in lateral view	18.52mm
Left coracoid maximal width in lateral view	?

1

Table 4(on next page)

Measurements of *Pulaosaurus qinglong* V30936 forelimbs.

Left humerus length in anterior view	50.16mm
Distal end width of left humerus in anterior view	10.86mm
Proximal end width of left humerus in anterior view	?
Shaft minimal width of left humerus in anterior view	6.04mm
Left ulna length in anterior view	40.86mm
Distal end width of left ulna in anterior view	7.30mm
Proximal end width of left ulna in anterior view	10.12mm
Shaft minimal width of left ulna in anterior view	4.92mm
Left radius length in anterior view	39.24mm
Distal end width of left radius in anterior view	6.76mm
Proximal end width of left radius in anterior view	6.24mm
Shaft minimal width of left radius in anterior view	3.40mm
Right ulna length in posterior view	43.24mm
Distal end width of right ulna in posterior view	5.4mm
Proximal end width of right ulna in posterior view	9.24mm
Shaft minimal width of right ulna in posterior view	4.04mm
Right radius length in posterior view	41.8mm
Distal end width of right radius in posterior view	6.7mm
Proximal end width of right radius in posterior view	5.48mm

Right radius shaft minimal width in posterior view	3.58mm
Left manual portion length	32.5mm
Longest left manual digit(2^{nd} digit) length	29.76mm
Left metacarpal I length	7.62mm
Left metacarpal II length	13.08mm
Left metacarpal III length	12.19mm
Left metacarpal IV length	8mm
Left metacarpal V length	5.36mm

1

Table 5(on next page)

Measurements of *Pulaosaurus qinglong* specimen V30936 pelvic girdle.

Total length of the ilium	69.84mm
Depth of the blade above the acetabulum	18.88mm
The width between the rostral margin of the pubic peduncle and the caudal margin of the ischial peduncle at the base	23.62mm
Preacetabular process length	28.08mm
Postacetabular process length	21.90mm
Postacetabular process depth	21.16mm

1

Table 6(on next page)

Measurements of *Pulaosaurus qinglong* V30936 femora, tibiae and fibula.

Left femur length in medial view	88.52mm
Proximal end width of left femur in medial view	14.04mm
Distal end width of left femur in medial view	14.68mm
Shaft minimal width of left femur in medial view	11.80mm
Right femur length in medial view	80.94mm
Proximal end width of right femur in medial view	?
Distal end width of right femur in medial view	16.24mm
Shaft minimal width of right femur in medial view	?
Left tibia length in anterior view	97.84mm
Proximal end width of left tibia in anterior view	20.02mm
Distal end width of left tibia in anterior view	?
Shaft minimal width of left tibia in anterior view	10.94mm
Right tibia length in medial view	98.76mm
Proximal end width of right tibia in medial view	20.44mm
Distal end width of right tibia in medial view	16.98mm
Shaft minimal width of right tibia in medial view	9mm
Left fibula length in anterior view	94.90mm
Proximal end width of left fibula in anterior view	2.68mm
Distal end width of left fibula in anterior view	7.3mm

Shaft minimal width of left fibula in anterior view	1mm

1

Table 7 (on next page)

Measurements of *Pulaosaurus qinglong* V30936 metatarsals and pedal digits.

Left/Right	digit	perspective	Length/mm	Proximal end width/mm	Distal end width/ mm
Right	Metatarsal I	anterior	27.68	?	5.64
Right	I-1	anterior	16.23	5.36	3.61
Right	I-2	anterior	10.06	4.66	/
Right	Metatarsal II	anterior	47.10	6.58	4.86
Right	II-1	anterior	16.82	7.44	4.96
Right	II-2	lateral	14.5	6.46	4.7
Right	II-3	lateral	12.9	5.28	/
Right	Metatarsal III	anterior	53.86	5.6	11.6
Right	III-1	posterior	15.68	11.42	8.04
Right	III-2	posterior	12.28	8	6.78
Right	III-3	posterior	12.34	8.12	7.22
Right	III-4	posterior	15.66	6.22	/
Right	Metatarsal IV	anterior	?	6.42	?
Right	IV-1	anterior	?	?	5.48
Right	IV-2	lateral	8.86	6.44	4.22
Right	IV-3	lateral	7.96	5.6	5.02
Right	IV-4	lateral	6.6	5.16	3.74
Right	IV-5	lateral	11	4.32	/
Left	Metatarsal II	posterior	47.28	8.32	7.42
Left	II-1	posterior	16.46	5.72	5.32
Left	II-2	anterior	?	8.2	?
Left	II-3	anterior	12.8	3.22	/
Left	Metatarsal III	posterior	54.36	6.92	9.52
Left	III-1	anterior	18.06	8.32	7.62
Left	III-2	anterior	14.71	8.28	7.36
Left	III-3	lateral	12.72	6.5	5.5
Left	III-4	lateral	16.36	5.41	/
Left	Metatarsal IV	posterior	66.04	8.52	5.56
Left	IV-1	anterior	11.53	7.52	6.08
Left	IV-2	anterior	8.9	5.53	5.38
Left	IV-3	anterior	8.6	4.92	4.26

Left	IV-4	lateral	7.32	4.48	4.28
Left	IV-5	lateral	12.04	5.90	/

1